

HIDDEN SPACE ENERGY

**THE HETERODYNE RESONANCE MECHANISM:
THEORY AND EXPERIMENTS**

(Extraction: Introduction, Chapter 7 about an overunity device and author biography.
The book is available in [amazon.com](https://www.amazon.com))

STOYAN SARG, Ph.D.

Copyright © 2020 by Stoyan Sarg. All rights reserved.

Fair Use Notice: The book contains a few figures, from peer-reviewed journals, and public domains. Such material with proper citation and acknowledgement is included with a purpose of scientific research, comments and criticism in effort for deeper understanding the laws of Physics. We believe this constitutes a 'fair dealing' and 'fair use' of any such copyrighted material as provided in Part III Section 29 of the Canada Copyright Law and section 107 of the US Copyright law.

Image on the book covers:

- Front cover: Picture of the author.
- Back cover: Pictures of glow discharge cells with activated HRM effect and one spectral band

CONTENTS

HIDDEN SPACE ENERGY	1
THE HETERODYNE RESONANCE MECHANISM: THEORY AND EXPERIMENTS	1
Acknowledgements	9
Disclaimer.....	10
INTRODUCTION	11
CHAPTER 1	13
THE CONTROVERSIAL ISSUE OF PHYSICAL VACUUM ENERGY FROM A NEW POINT OF VIEW.	13
 1.1. Historical overview	13
 1.2. A new space concept according to the BSM-SG unified theory	15
 1.3. Energy of the physical vacuum and its relation to velocity of light from the viewpoint of BSM-SG unified theory.....	19
CHAPTER 2	25
DIFFERENCE BETWEEN BSM-SG ATOMIC MODELS AND QUANTUM MECHANICAL MODELS OF THE ATOMS AND ELEMENTARY PARTICLES	25
 2.1. Problems with the quantum mechanical models. Why do they use energy levels only?.....	25

2.2. Physical models of elementary particles and atoms derived in BSM-SG theory.	28
2.3. Structure and oscillating properties of the electron and its interaction with the CL space.....	32
2.4. Quantum mechanical properties of the electron as specific interactions with the oscillation features of the CL nodes.....	35
2.5. Internal energy of the electron related to its oscillation property.	41
2.6. Rydberg state of the atoms and ion-electron pair.	42
CHAPTER 3	45
PHYSICAL APPROACH FOR ACCESSING THE ZERO POINT ENERGY PREDICTED BY THE BSM-SG UNIFIED THEORY.....	45
3.1. Important questions about Zero Point Energy.	45
3.2. Access to the ZPE-S (static ZPE).....	45
3.3. Accessing the ZPE-D (dynamic ZPE).	48
3.3.1. Physical and technical overunity and source of energy	48
3.3.2. Physical mechanism of interaction with the CL space (quantum interaction).	49
CHAPTER 4	52
HETERODYNE RESONANCE MECHANISM (HRM). THEORY AND EXPERIMENTAL STUDY.	52

4.1. Heterodyne Resonance Mechanism in electro-magnetically activated plasma.	52
4.2. History of Rydberg matter study in plasma.....	55
4.3. Considerations for invoking the Heterodyne Resonance Mechanism	56
4.4. Heterodyne Resonance Mechanism in a glow discharge phenomenon.....	58
4.5. Experiments for studying the physical properties of the Heterodyne Resonance Mechanism.	62
4.5.1. Vacuum cells	62
4.5.2. Basic circuit setup for study of the HRM effect	64
4.5.3. Experimental results.	67
4.5.4. Analysis of the experimental results. Physical characteristics of the HRM effect.	77
4.6. Conclusions from analysis of the experimental results.....	83
4.7. Analysis of prior art research on Rydberg matter showing the signature of HRM effect.	85
CHAPTER 5	88
ENERGY OF LIGHTNING.....	88
5.1 Observations and study of lightning phenomena..	88
5.2. Polarity and phase of lightning hitting the ground. Signature of the HRM effect.....	88
5.3. Time evolution of the lightning hitting the ground	91
5.3.1 First phase:	92

5.3.2 Second phase.....	93
5.4 Observed lightning features not explained so far.	96
5.5. The Heterodyne Resonance Mechanism (HRM) in lightning.....	96
5.6. A method for a laboratory-invoked lightning phenomenon	99
5.7. A laboratory equipment for study of lightning phenomenon.	100
5.8. Conclusions:.....	102
CHAPTER 6	103
HISTORICAL OVERVIEW OF DEVICES AND EXPERIMENTS FOR ACCESSING ZERO POINT ENERGY.	103
Experimenters and inventors of devices with identified signature of the HRM effect.....	103
6.1. Nikola Tesla.....	103
6.2. Thomas Henry Moray	106
6.3. Paul Bauman.....	107
6.4. Analysis of Testatika machine and principle	109
6.5. Joseph (Josef) Papp.....	114
6.6. Papp noble gas engine: How it works.	116
CHAPTER 7	127

PHYSICAL AND TECHNICAL CONSIDERATIONS FOR ACCESSING THE ZERO POINT ENERGY BY THE HRM EFFECT	127
7.1. Considerations and technical requirements for using the HRM effect.	127
7.2. The Papp engine and related experiments.	128
7.2.1. Physical and technical considerations	128
7.2.2. Physical and technical overunity	131
7.3. Experimental setup.....	133
7.3.1 Plasma ignition device	133
7.3.2. Electrical system.....	137
7.3.3. Vacuum/gas filling system	145
7.3.4. Block diagram of the complete test system.....	147
7.3.5. Calculation of distances between HV electrodes....	147
7.4 Energy measuring system and test procedure	148
7.4.1. Measuring of the input energy:.....	148
7.4.2. Measuring of output kinetic pulse energy:	149
7.5. Example of energy efficiency estimation using the data published by Bob Rohner for his Plasma Blaster device	152
7.5.1. Input energy for a single plasma expansion pulse .	152
7.5.2. Output energy from the single plasma expansion pulse.	153
7.6. Conclusions and technical recommendations for researchers.	155
7.7. Considerations for technical overunity	156
7.7.1 Kinetic to electrical energy conversion.....	156
7.7.2 Estimation of necessary efficiency of the Plasma device for obtaining net output energy (power).	158
7.7.3. Twin piston device with linear generators.....	164

7.8. Summary and general conclusions	166
AUTHOR BIOGRAPHY	169
GLOSSARY	172
REFERENCES:	174

Acknowledgements

I wish to express my thanks to a wide circle of people with whom I communicated for about 20 years, even before my first publication of the treatise BSM - Supergravitation Unified Theory in 2001. During all those years of research and experimentation, I was in contact with many scientists at different institutions. I am thankful to Acad. Dr. Prof. Asparuh Petrakiev – a recognized scientist who first noticed the novelty and importance of my treatise. He provided a valuable scientific review and supported the work with seminars. My special thanks to Dr. Andrew Michrowski, a President of the Planetary Association for Clean Energy, Inc., Canada, for the encouragement, moral support and useful connections I had for many years. I would like to express my appreciation to the Board of Directors of the World Institute for Scientific Exploration for the encouragement and support of my theoretical research and providing opportunities for conference presentations. I highly appreciate the help of William Treurniet for editing the English edition of this and other books, and for useful discussions and suggestions. I am thankful to Acad. Prof. Dr. Yachko Ivanov and Prof. Dr. Rumen Kakanakov from the Bulgarian Academy of Sciences for their help in publishing a short version of my theory in Bulgarian language titled “Matter, Space, Gravitation”. I thank my technical assistant, Velin Asenov, who was always ready to build experimental devices with a firm belief that the stated goal would be reached. I would like to express my appreciation to my former colleagues, scientists, professors and technical staff at York University, Toronto, Canada for the moral support of experimental work that was usually not officially funded. I appreciate the patience, moral support and encouragement of my wife Denka and son Ivor given the enormous amount of time I devoted to this work.

Disclaimer

The access to hidden space energy by the Heterodyne Resonance Mechanism is a new field of research that may involve some unknown side effects. Experimenters in this field must take special precautions. From one hand they must use high voltage in the order of 40 – 60 kV. From the other hand the effect is accompanied with emission of Longitudinal (referenced also as Scalar) waves. Isotropic Longitudinal waves dissipate fast with the distance but may penetrate through shields and can propagate by ground connections. They may cause problem for sensitive electrical equipment. For this reason, the power supply source must be from a battery that is completely separated (no galvanic connection) from the power grid. For measurement of electrical parameters electromagnetic instruments are preferable or if using digital instruments they must be optically isolated. If using a power above a few hundred watts the experimenters must be cautious about some unknown health effects. Individual researchers must be aware that they provide experiments in this field at their own risk and responsibility. The author of this book cannot be held responsible for any injury, damage or loss of property that may eventually occur by improper experimental setup or test provided in not suitable environment.

INTRODUCTION

Our curiosity for understanding the Universe has presented us with an illogical absurdity. How could the Universe begin with an explosion from a singularity (a mathematical point) and continue to expand with a velocity approaching the speed of light? Where did this unimaginable enormous energy come from? Today we often hear of concepts like the existence of dark matter, dark energy, and even a negative energy. What is the physical meaning of these absurd concepts? Are they a result of something fundamentally wrong about our view of the space we live in?

Dissatisfaction with such absurdities led me to search for the fundamental truth. For many years I reviewed articles in quite different fields before arriving at an original idea on space, time, matter and energy. In 2001 I published the treatise Basic Structures of Matter – Supergravitation Unified Theory (BSM-SG). Reviving the old belief of the existence of a space medium, I elaborated a detailed space-time physical model I called the Cosmic Lattice. Such a model has never been investigated before. This was a starting point from which I succeeded in building physical models of elementary particles. This permitted a new logical understanding of accumulated knowledge about physical phenomena in quite different fields of physics.

The new space-time concept of the BSM-SG theory revealed the heretofore unpredicted existence of hidden space energy. It is related to the controversial issue of Zero Point Energy (ZPE). Although particle physics experiments and some elaborations in quantum mechanics lead to the possible existence of such energy, its physical origin was an unresolved enigma. The reason is the denial of the existence of a space medium. In fact, its existence is hidden behind meaningless terms like “physical vacuum”, “space-time”, “vacuum polarization”, “quantum phenomenon”, etc. A frequent tendency today is to assign the term ‘quantum’ or use the uncertainty principle as a cover for phenomena for which there is no reasonable explanation. The BSM-SG theory demonstrates that a logical explanation does exist for any physical phenomenon.

Using the BSM-SG models for experimental analysis, I found that the existence of a space medium is fundamentally important for understanding with unperturbed human logic all processes from the micro-cosmos to the universe. It defines not only the velocity of light, but also Newtonian gravitation, mass and inertia, the electrical and magnetic fields, the quantum mechanical properties and relativistic effects. Furthermore, the unveiled structure of space called the Cosmic Lattice, contains two forms

of hidden space energy – static and dynamic. They are spread everywhere in the universe around us. The static energy is the primary source of nuclear energy, while the dynamic type is the enigmatic ZPE. The latter type is behind the electrical and magnetic fields. It is much weaker than the static type but is also unlimited because the two types are connected. This energy is not a form of radiation. A fraction of this energy can be accessed by a physical phenomenon that I discovered and called a Heterodyne Resonance Mechanism (HRM). The HRM effect was successfully used in my research on gravity, described in the book, “Field Propulsion by Control of Gravity – theory and experiments”, published in 2008. I was convinced at that time that the HRM effect could also be used to access the ZPE, but some time was needed for experimenting and elaboration of the technical means.

In this book I teach how to use the HRM effect for accessing the hidden ZPE. Obtaining a fraction of this energy can be achieved only following a clear understanding of the underlying physical process. This book creates the opportunity for beginning a completely new direction of research in which the power of logical understanding will demonstrate unexpected results.

I would like to mention that access to this hidden space energy might possibly be accompanied by some unknown effects. My advice is to try initially no more than couple hundred of watts power. Jumping to higher power could require the use of some radioactive isotopes. For these and other reasons, my opinion is that the goal is to build small energy devices. Their independence from natural resources, for example, will make them useful for space environment. This might be beneficial for humanity. How will the Earth handle its growing population? Our civilization may reach the point of exhausting the Earth resources. This could lead to wars for resources and finally to ecological disaster. Even without a global war or pandemic event the tendency to replace natural resources with artificial might have unpredictable side effects for human health and environment. A new direction of research based on the discovered HRM effect could lead to new technologies suitable for a space travel.

The price of this e-book is fairly low for the useful information it provides. My whole life experience is behind it. The advice to the reader who plans to do experimental work is to buy also the paperback version. The latter is more convenient as a frequent reference manual where one could put own marks.

Stoyan Sarg, Canada, 2020.

CHAPTER 7

Physical and technical considerations for accessing the zero point energy by the HRM effect

7.1. Considerations and technical requirements for using the HRM effect.

The conclusions in §4.55. of Chapter 4 are quite important for understanding the physical process of lightning. Conclusions 3 and 4 of §5.8 from the analysis of lightning are also of particular importance. They help to understand the conditions for releasing the energy accumulated in the superclusters of ion-electron pairs. Not all ionized atoms can be involved in the formation of ion-electron pairs. Some of them will contribute to current. If this current exceeds some critical level, the generated magnetic field will affect the complex magnetic field of the ion-electron pairs (see §4.5.4 and §4.5.5). This could lead to their destruction and the release of the zero point energy accumulated in them. The process is developed as an avalanche. The observed effect is a rapid gas expansion (thunderstorm), optical flash and EM radiation.

It is evident that there are not directly observable physical sub-processes in lightning phenomenon and three apparent effects.

Not observable physical sub-processes:

- a. Creation of ion-electron pairs and accumulation of zero point energy**
- b. Destruction of the superclusters of the ion-electron pairs and release of the accumulated zero point energy.**

Apparent effects:

- c. Gas expansion (and contraction in Papp's engine)**
- d. Optical flash and thunder**
- e. EM radiation**

These effects are identifiable also in the Papp engine, in Edwin Grey's power tube and in the Testatika machine developed by Paul Baumann.

Physical sub-process a.

In the case of the natural lightning phenomenon, the ion-electron pairs are the result of the ionization process causing the electrification of the clouds [89]. They are distributed in a large volume.

In the case of Papp's engine, the ion-electron pairs are also a result of ionization but caused by radioactive isotopes and RF emitters in the MHz range. The spark discharge also creates ionization and formation of ion-electron pairs, but in a small volume surrounding the spark. In our small volume experiment, this could be done either by using radioactive isotopes (enclosed in "buckets"), and RF or microwave radiation within a proper spectral range. It is a good idea to avoid initially the use of radioactive isotopes in the experiments and devices. The ionization can be achieved by other means, but the technical solution requires more experimental research. The advantage of using radioactive isotopes is more uniform volume ionization, but there is a danger of radioactive contamination.

Physical sub-process b.

The destruction of the ion-electron pairs is achieved by injecting a strong current through the plasma. The magnetic field of this current interacts with the magnetic field of the ion-electron pairs. This leads to their full or partial destruction and the release of the stored ZPE energy accessed by the electrons. In fact, the technical realization of the HRM effect appears implemented in the Papp engine described in the patents, although the inventor lacked the physical understanding. The electrical part of the implementation includes a plasma switch discussed in section §7.3.

7.2. The Papp engine and related experiments.

7.2.1. Physical and technical considerations

The working effect in Papp's engine and similar experiments is the process of gas expansion and contraction. We may call it a plasma ignition. An external magnetic field generated by a solenoid is implemented in Papp's engine and most of the other replication

devices, but without physical understanding of its role. The experimenters mention that this increases the displacement of the piston from the gas expansion. In fact, such an effect is in complete agreement with the theoretical considerations d. in §4.5.5. The use of an axially aligned external magnetic field helps to orient the ion-electron superclusters in the direction of gas expansion. This contributes to the non-thermal expansion effect of the expanding gas. Another feature of the superclusters is also very important: the RF emission and also the collision properties of the Rydberg matter. This is in agreement with the study of L. Holmlid [25] and F. Olofson, P. Andersson and L. Holmlid about Rydberg matter (ion-electron pairs): *the time between collisions of RM clusters with gas molecules is approximately 100ns, while the time between collisions with other RM clusters is > 6 hrs.* [27]. This is an extremely important signature of the strong stability of the superclusters of ion-electron pairs. Therefore, their orientation by an external magnetic field is quite important prior to the gas expansion. Then the gas expansion exhibits a strong unidirectional pressure component. This, in fact, contributes to a unique non-thermodynamic effect and explains why an insignificant temperature rise is observed in the experiments using Papp's principle.

One particular feature of the HRM effect that is not envisioned either in Papp's or other patent applications should be emphasized. In the experimental study and analysis in §4.3 and particularly in Fig. 4.12, it was found that the HRM oscillations are separated from the activation pulse by a specific time delay. This delay was about 20 uS in the test at partial vacuum, but it might be different for different gases and gas pressures. It could depend also on other technical design parameters. These conditions are difficult to predict, but the delay is important. This could perhaps have been one of Papp's problems. The time from his first successful prototype until his death was about 20 years. However, he was unable to achieve the expected efficiency in successive prototypes built during that time. Other experimenters on Papp's engine also did not envision the importance of such a physical parameter. The optimal delay must be found by following the test procedure.

From the physical point of view we formulate the following considerations:

- 1. Creation of ion-electron pairs in a possibly large volume:**
 - a.** by using a high voltage with a broad frequency range to ionize the gas mixture
 - b.** by using radioactive isotopes enclosed in capsules of a properly selected metal with a proper thickness.
- 2. Use of a high current from a low voltage source to destroy the ion-electron pairs in order to release the stored zero point energy**
- 3. Use of an external magnetic field for proper orientation of the superclusters of ion-electron pairs.**
- 4. Implementation of an adjustable delay between the triggering HV spark and the low voltage high current**
- 5. Use of a technical means for conversion of the plasma expansion to usable energy**

Consideration 1. a. could be technically realized by using a Tesla coil with a spark gap. It generates HV pulses with a broad frequency spectrum. The spark could be AC or could be rectified by fast HV diodes and must trigger a corona effect. The technical problem with this option is the uniform creation of ion-electron pairs in a large volume, since the corona effect depends on gas pressure and surface contamination.

Consideration 1. b. This option, used in Papp's patent and other patent applications, assures more uniform ionization in the working volume. It is not affected by the surface contamination. The use of radioactive isotopes, however, puts some restrictions on the design of commercial devices.

Consideration 2. It is preferable to use the discharge of a charged capacitor. The initial current is quite strong and falls exponentially. This is useful from the point of view of decreasing the input energy.

Consideration 3. A cylinder with a piston made of non-magnetic material would convert the expanding gas plasma to mechanical energy.

Consideration 4. There are two options for realizing the required magnetic field: **a.** an external solenoid coil supplied by high current; **b.** a permanent magnet.

In case **a.** the coil should contain a large number of turns of a proper wire diameter. The current through the wire should be constant during the gas expansion phase. (In Bob Rohner's Plasma Blaster, the current from 24 VDC is about 3-4 amperes).

In case **b.** the magnet should be of ferrite type in order to avoid an eddy current.

Consideration 5. The delay between the HV spark and the beginning of current discharge of a capacitor must be tuned during the operation until the optimal efficiency is reached.

The process of plasma expansion and contraction exhibit some important features not envisioned by classical thermodynamics. It does not cause a temperature increase like in fuel combustible engine (only a few degrees). This effect is more apparent when operating with a mixture of noble gases than with air. It has been demonstrated by a number of experimenters and especially by Bob Rohner. Our conclusion is that two physical processes are involved in the gas expansion and collapse: **one is a classical thermodynamic process, but the other is not.**

A part of the input energy is spent in a thermodynamic process. It is transmuted to heat and so a small portion is used for gas expansion. This is the classical thermodynamic process.

The remaining input energy goes to creation of ion-electron pairs. **It triggers the process of tapping the zero point energy which is not a classical thermodynamic process. The orientation of the superclusters by the external magnetic field is also a non-classical thermodynamic effect.**

7.2.2. Physical and technical overunity

According to the brief introduction in §3.3.1, physical overunity is considered for input and output energies of different kinds (for example, electrical input energy and kinetic output energy), while technical overunity means that both energies are of the same type. The preferable option is for both to be of the electrical type.

In the case of Papp's engine principle, physical overunity is the initial goal, without which technical overunity is impossible. Obtaining a plasma expansion is not a problem, but physical overunity could not be achieved without optimization. Such optimization is possible only by understanding the underlying physics.

Obtaining overunity requires the energy of the non-thermodynamic effect to be greater than the energy of the thermodynamic effect.

The non-thermodynamic effect of gas expansion should be optimized in order to achieve overunity. The external magnetic field plays an important role for this purpose.

Question: Why does the gas contraction appear slower than the expansion?

The theoretical answer is the following. The axially oriented clusters of ion-electron pairs contribute to the gas expansion in the direction of piston motion. At the end of the expansion phase, they are destroyed and don't have the property of their own magnetic field. Consequently, they could not possibly be oriented along the external magnetic field. So the contraction phase will not have the same unidirectional property as the expansion phase. In other words, in the contraction phase the classical thermodynamic effect dominates.

If a minimum physical overunity is obtained, the following considerations are valid for achieving technical overunity.

- a. **Use of a means for converting gas expansion to a kinetic mechanical energy**
- b. **Use of a means for converting mechanical into electrical energy**
- c. **Use of an electrical converter to supply the required input electrical energy obtained from a fraction of the output energy.**

The cases a. and b. are implemented in Papp's engine and in other patents mentioned in §6.1.1. There is no existing information for the implementation of case c. In the Testatika device of Paul Baumann, a different technical implementation is used for capturing the zero point energy and converting it into current.

7.3. Experimental setup.

The main purpose of this book is to guide experimenters and researchers. There is a useful parallel between the physics of natural lightning and the concept of Papp's engine. Before jumping to build a device with technical overunity, it is preferable to create an experimental setup in which the input and output energies can be estimated with a high level of confidence. During the tests, important theoretical understanding and practical experience would be obtained.

The experimental setup includes a Plasma ignition device comprised of mechanical and electrical parts, a vacuum pump, a gas filling system and a measuring system. The Plasma ignition device helps to understand the functional operation of Papp's engine, to estimate input and output energy, and to provide important measurements and adjustments of some critical parameters.

7.3.1 Plasma ignition device

Fig. 7.1. shows a model of a test bed that will help understanding the principle of Papp engine. Some differences from Papp's engine model will be mentioned below.

The cylinder 1 and the piston 2 are made of non-magnetic material. The piston has a stop position at its left-most position that defines the initial volume of the working chamber 3. The chamber is initially purged by a vacuum pump through a valve 8 and then filled with an noble gas mixture.. The gas mixture is at normal atmospheric pressure, but optionally it could be at a higher pressure.

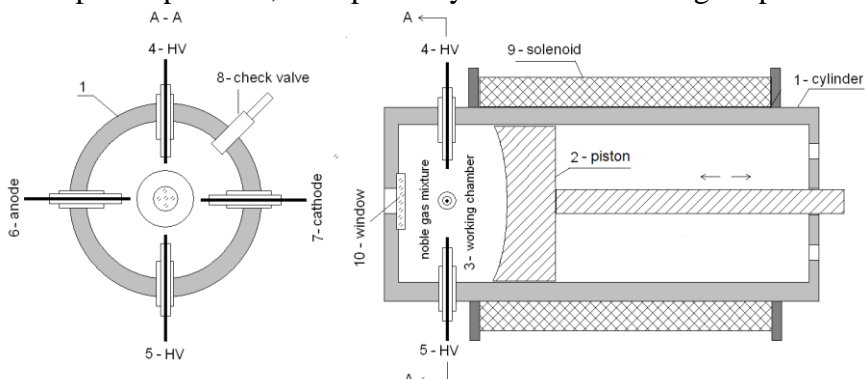


Fig. 7.1. Functional model of the Plasma ignition device

The solenoid 3 contains many turns of a thin wire with a purpose to create a homogeneous magnetic field inside of the working chamber. The electrodes 4 and 5 are for the high voltage spark, while the electrodes 6 and 7 are for the low voltage high current discharge from a capacitor. All four electrodes are of tungsten, and the anode and cathode do not contain any radioactive isotopes. Initially, a HV on the order of 40 kV is applied (AC or DC), usually as multiple pulses to electrodes 4 and 5. A thin plasma discharge appears between the electrodes, but it must pass through the four electrodes. Usually, a relay can connect the anode and cathode to a capacitor and a strong current is discharged through the plasma. (However, the author performed successful experiments without a relay). At this point, an explosion is observed causing a Plasma expansion followed by immediate contraction. The piston is displaced and then returned to the initial position. The Plasma expansion from the explosion seems less sudden than from a chemical explosion and is followed by immediate contraction. Also, the expansion time is shorter than the contraction time. When the solenoid coil is activated, the expansion is stronger. Many researchers have pointed out that the process does not deliver much heat in comparison to the fuel ignition in a gas combustion engine.

The configuration of the electrodes plays the role of a plasma switch. The HV spark creates plasma through which the current from a low voltage source passes. In fact the HV spark creates initially plasma of ion-electron pairs and then the strong current from the capacitor discharge causes the ignition of the plasma. This is a short transient process causing increase of the pressure followed by a slower decrease. In Pap's engine a radioactive source and RF emitter are used for the gas pre-ionization (creation of ion-electron pairs). We do not use any radioactive source. The low voltage usually comes from a charged capacitor, but a minimum voltage threshold is required. It could be in the range of 100 to 500 VDC, depending on the capacitor value and electrode configuration and gaps. When the time between consecutive HV triggering is decreased, the plasma ignition occurs at a lower voltage because of the residual ionization.

In an experimental setup for studying the process for achieving overunity, it is useful to replicate the device built and demonstrated by Bob Rohner known as the Plasma Blaster (fig. 6.7), but with some functional improvements. Bob Rohner does not have his own patent, but his research and development of a variety of devices based on Papp's principle was quite useful in the analysis. The picture of the Plasma Blaster built by Bob Rohner was shown in Fig. 6.8.a, while the bottom head with electrodes was shown in Fig. 6.8.b (Chapter 6).

In 2018-19, the author and technical assistant, Velin Asenov, built and tested an experimental plasma ignition device. It is similar to Bob Rohner's Plasma Blaster but has some modifications. The mechanical part of the device is shown in Fig. 7.2. a. and the electrode system in Fig. 7.2.b. The device must be fixed on an elevated stand in order to observe the flash of plasma through the bottom window through a 45 deg mirror. (This arrangement is used by Bob Rohner). The bottom section, called a head, encloses a working chamber with permanent magnets and an electrode system. The noble gas mixture passes through the check valve 8 after the working chamber is purged by a vacuum pump. The cylinder at the top of the head contains a piston. A rod extends above the cylinder that can push another rod connected to a measuring system. The following modifications differ from the Plasma Blaster of Bob Rohner. Instead of an external magnetic field created by a solenoid placed over the working cylinder, two permanent magnets inside the working chamber were used. A ring spacer of soft iron was placed between the magnets in order to extend the magnetic field. A homogeneous magnetic field is created inside of the working chamber , aligned along the axis of the cylinder.

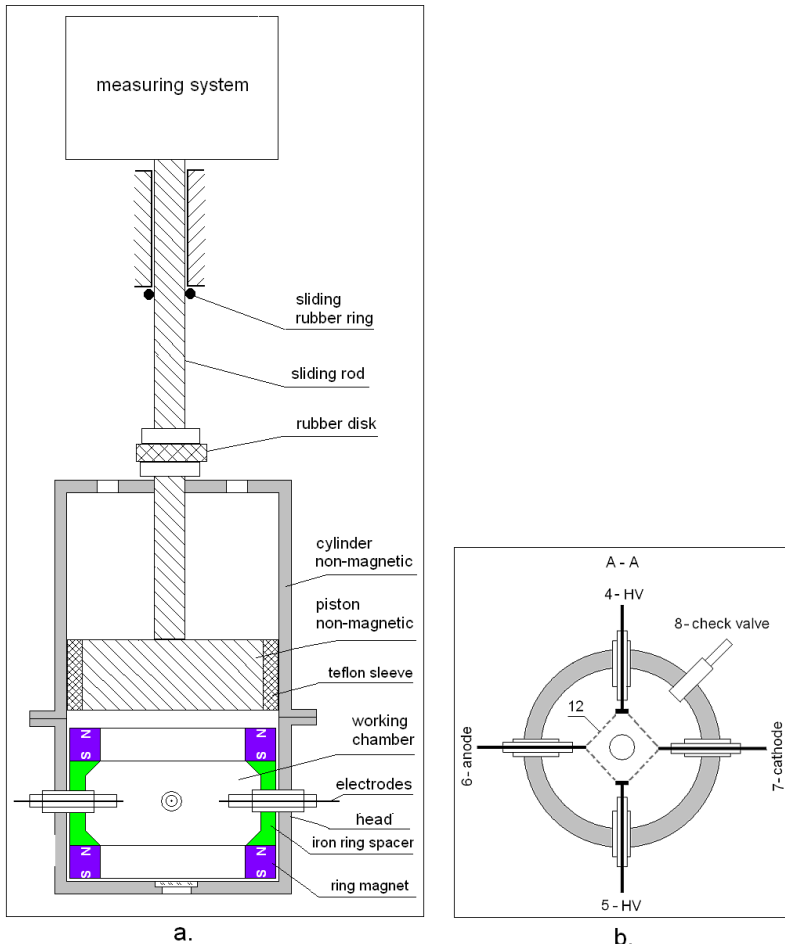


Fig. 7.2. Sketch of the experimental Plasma ignition device;
a. – mechanical part, b.- electrode system.

A small modification was also made in the electrode system. In order to avoid a direct HV discharge between the electrodes 4 and 5, the tips of these electrodes have the configuration shown in Fig. 7.2.b. In this case, the high voltage spark has a path 12. It must connect all four electrodes in order to provide conductive plasma for the strong low-voltage current from the low-voltage source (charged capacitor) in order to pass between the anode and cathode. This is a kind of plasma switch which is activated by the HV spark.

In prior art experiments the high and low voltage discharge are separated by a relay. The relay usually has a delay in milliseconds. Consequently, the logic that controls the necessary delay according to Consideration 5 must take this into account. It also puts a rigid constraint on a small jitter from the relay. Other options without using a relay are possible for those who have the necessary skill. The author designed a plasma switch that allows the delay to be adjusted without using a relay. The circuit is shown and discussed in the next section.

7.3.2. Electrical system

The electrical block diagram designed by the author for the experimental plasma ignition device is shown in Fig. 7.3. The picture of the electrical block was shown in Fig. 5.6 (Chapter 5). (Bob Rohner does not provide the electrical circuit of his Plasma Blaster).

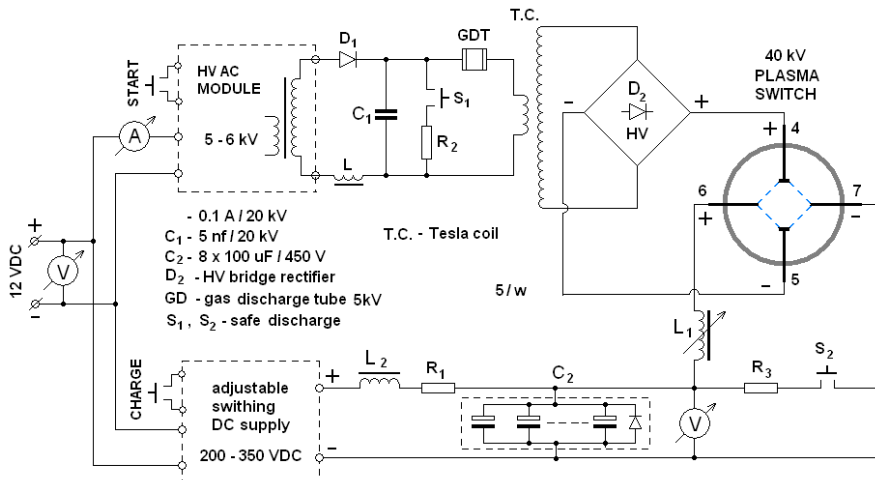


Fig. 7.3. Electrical block (circuit) diagram of the experimental plasma ignition device

The capacitor bank C_2 is initially charged to a selected voltage in the range of 300 – 380 VDC and then a HV spark is triggered by the start button. The capacitor C_2 discharges through the plasma switch with a loud sound, but C_2 does not discharge in full. It must also be mentioned that a minimal threshold voltage

exists, not only for HV but also for the voltage in the C_2 capacitor, in order to discharge through the plasma switch. In a successful triggering, the threshold of the C_2 voltage decreases slightly.

The HV AC module drives a Tesla coil T.C. through the circuit shown in Fig. 7.3. The circuit diagram of this module is shown in Fig. 7.4.

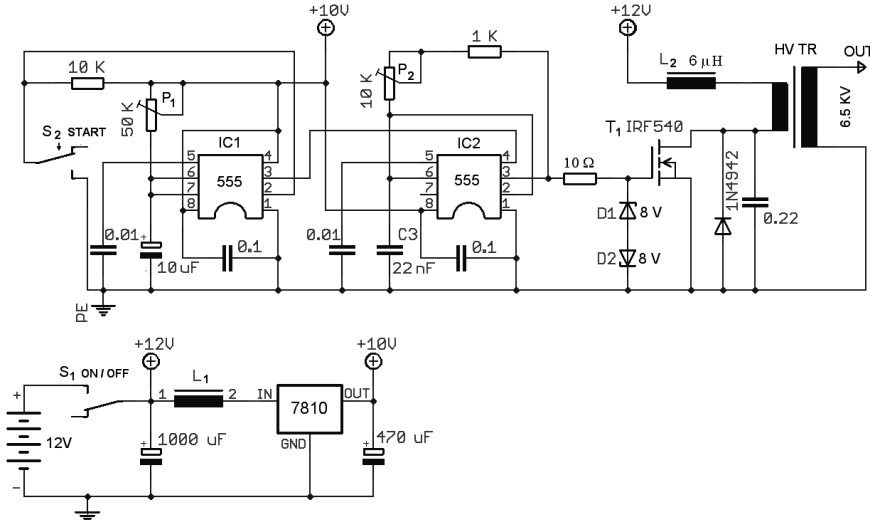


Fig. 7.4. Circuit diagram of HV AC supply module and Tesla coil driver.

The Tesla coil is wound on a tube with a diameter of 25 mm. It has a primary coil of 7 turns of thick 2 mm diameter wire and a secondary coil with 140 turns of 0.4 mm diameter wire. The inductance of the secondary is $267 \mu\text{H}$. The output of the Tesla coil is rectified by a HV diode bridge D_2 and conveyed to the HV electrodes 4 and 5. The HV bridge D_2 is comprised of 8 HV diodes – 2 diodes in each bridge arm connected in series. The main specifications of the diodes are: 20 KV, 0.1 A, 100 ns. The HV spark through the plasma switch consists of HV pulses with amplitude of about 40 kV and repetition rate of 200 pulses/sec. On top of these pulses there are HV pulses with a frequency of 50 kHz. This frequency can be adjusted by the potentiometer P_2 (Fig. 7.4), while the pulse rate is defined by the circuit C_1 and the voltage value

of GDT and L_1 (Fig. 7.3). GDT is known also as a surge arrester. It is for 5 kV and serves as a spark gap for the Tesla coil.

The shown electrical part permits operation of the Tesla coil for a time duration defined by IC1 after pressing the button S_1 . The mono-vibrator (one short) build on IC1 defines the ON time duration that is adjusted by the potentiometer P_1 . The 50 kHz frequency of the Tesla coil is defined by the multivibrator IC2 and the frequency is adjusted by the potentiometer P_2 .

The HV transformer is a model 28K047 from www.amaizing1.com. Such a transformer could be also built on a ferrite core used in old CRT monitors with proper isolation of the secondary coil. The inductance L_2 must be on a ferrite core with an air gap (mica spacers). The presented driving circuit of the Tesla coil provides very high-power efficiency, about 90%.

The low voltage section contains a capacitor charger that is a DC supply module with adjustable output between 100 and 400 VDC. It charges a capacitor bank of 8 electrolytic capacitors, 100 m μ F/450 V, connected in parallel. The inductance L_1 with a value of about 0.5 – 1 mH, together with the resistor R_1 (Fig. 7.3), is needed to limit the initial peak current during charging of the capacitor. The resistor R_1 is preferably a power wired resistor in the range of 20 to 100 ohms depending on the required rate of consecutive triggerings. The capacitor charger could be a commercial one; however, it must be of a switching type with proper parameters to avoid energy loss in some heated elements. Alternatively, it could be built as a flyback transformer with a rectifier. To have an effective power, it must operate at a frequency that resonates with the ferrite transformer. The author designed a capacitor charging module, and its circuit diagram is shown in Fig. 7.5.

The transformer is built on two U-core ferrites used in old TVs or computer monitors with a CRT. IC1 is an oscillator, the frequency of which may be adjusted to the ferrite resonance frequency. The voltage to which the capacitor bank must be charged depends on the time the switch S_1 is on. Note that the initial current in this circuit is high (about 5 A) for tens of milliseconds, so that for fast charging a lead acid battery of 12 V is suitable. For a smaller initial current, the value of R_1 (Fig. 7.3) could be increased at the expense of some power loss due to heating.

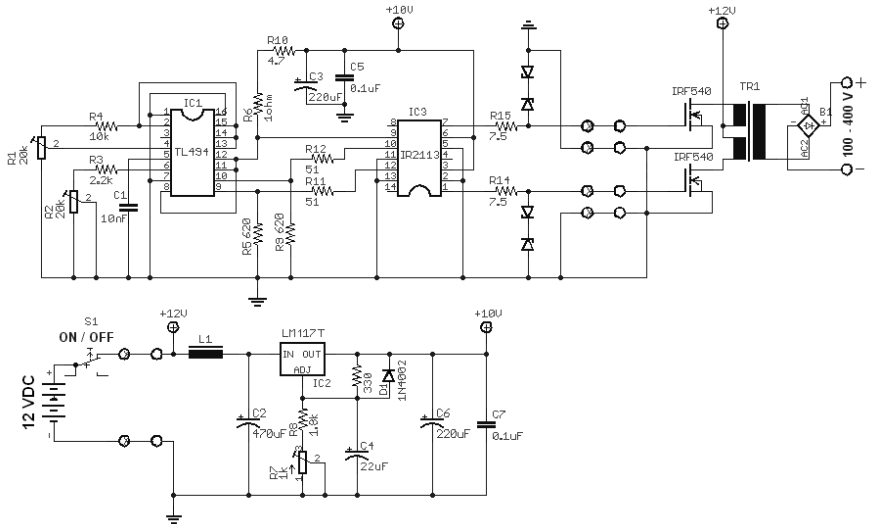


Fig. 7.5. Circuit diagram of a capacitor charger

Fig 7.6 shows the picture of the capacitor charger.



Fig. 7.6. Capacitor charger built on the circuit shown in Fig. 7.5

Fig. 7.7 shows a picture of the electrical part of the experimental plasma device.

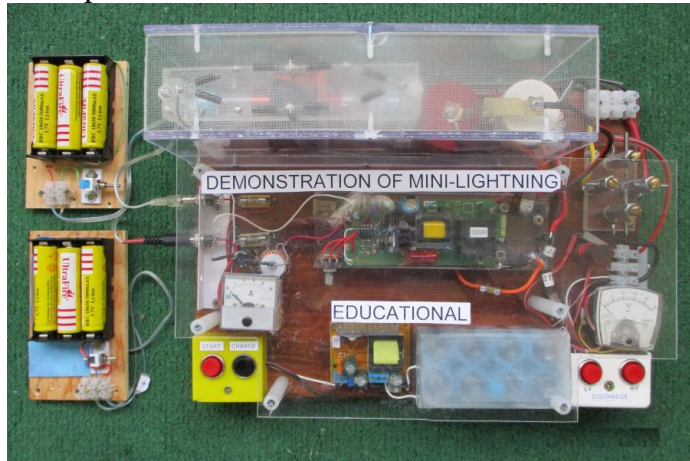


Fig. 7.7. Device for demonstration of mini-lightning. (A portable commercial module for charging the capacitor C_2 was used).

Fig. 7.8 shows the experimental system for the initial prototype of the plasma ignition device (electrical and mechanical) with the vacuum pump, gas filling system and measuring air pressure cylinder.



Fig. 7.8. Experimental system of the plasma ignition device shown with the author (right) and his technical assistant, Velin Asenov (left)

It must be pointed out that there is a critical time delay between the HV spark and the low voltage current found experimentally. It corresponds to the theoretical Consideration 5 in §4.55.a. Chapter 4. The delay is necessary to create ion-electron pairs and it must be adjusted experimentally. It was not envisioned by Joseph Papp and all other researchers, but it is critically important. The delay is implemented by the adjustable inductance



L_1 . It must be wound over an open ferrite core as shown in Fig. 7.9. (A coil with a ring ferrite should not be used because of saturation caused by the initial current from the capacitor discharge).

Fig. 7.9.

The ferrite core (from an old AM receiver antenna) is about 8 mm in diameter and 10 cm long. The coil contains 50 turns of 1.4 mm diameter copper wire. The inductance is adjustable in the range from 0.25 mH to 0.3 mH by sliding the ferrite core.

For studying Papp's engine principle, the demonstration of mini-lightning (Fig. 7.7) can be used, but it is not enough for obtaining the expected energy efficiency. Gas ionization from the HV spark is not sufficient for creation of the necessary quantity of ion-electron pairs. In Papp's patent, the low-voltage electrodes contain "buckets" of enclosed radioactive isotopes (see §6.1.1 and Fig. 6.2). They are also connected to a high frequency (HF) generator. According to Papp's patent, the generator is adjustable and generates a single frequency in the range of 26 to 40 MHz. Both the radioactivity and the HF radiation, combined with a proper gas mixture, assure a constant ionization below the level of the plasma conductivity. This is a condition for creating sufficient ion-electron pairs. In other words, the ionization must be below the level at which the plasma switch is triggered. Our experimental setup for the plasma device did not have such means and this obviously affected the efficiency. The single pulse output energy that we obtained was a few times smaller than the pulse energy of Bob Rohner's Plasma Blaster, but we did not have a radioactive source, a RF emitter and a noble gas mixture. Nevertheless, the effect of

plasma expansion and contraction, even with air at normal atmospheric pressure, was observed in all our tests.

In Papp's patent and Bob Rohner's Plasma Blaster, the RF source is conveyed to the anode or cathode or to both. Our suggestion is to use a Tesla coil with an air gap (or a glow discharge tube instead of air gap) that generates not a single, but multiple frequencies in the MHz range. Fig. 7.10. shows the circuit diagram of a self-oscillating low-power Tesla coil designed for this purpose.

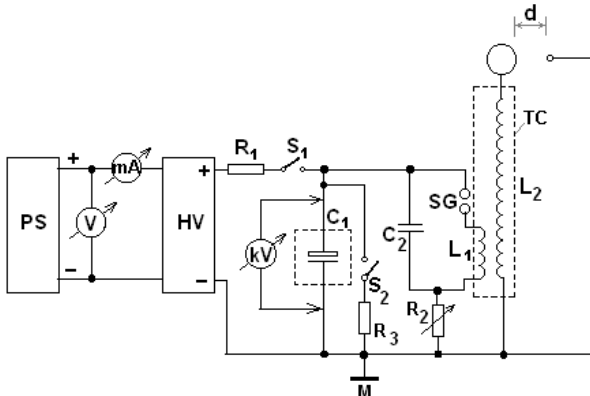


Fig. 7.10. Efficient low-power self-oscillating Tesla coil

The circuit of Fig. 7.10 is similar to the circuit for studying the HRM effect in plasma given in Chapter 4 (Fig. 4.21) but with some differences. Instead of the vacuum cell VC (Fig 4.21) there is an open air spark gap SG while the inductance L_1 is a primary of the Tesla coil TC. The capacitor bank is made of 12 capacitors, 100 μ f/450 VDC, connected in series. The ampere and voltage meters are for adjustment of the Tesla coil operation. R_1 is needed to limit the initial charging current of C_1 . The unique feature of this Tesla coil is that it is self-oscillating. Oscillations take place in the primary circuit SG, C_2 and L_1 at proper values of the HV, the spark gap SG distance, the capacitor C_2 and resistor R_2 . Depending on selection of the above-mentioned parameters, the oscillations in the primary coil are in the range of 30 – 200 Hz. They result from the negative slope of the V-A characteristic of the spark gap SG. At the secondary Tesla coil, oscillations are in a broad MHz frequency range covering the HRM spectra.

This self-oscillating Tesla coil is distinguished from the classical one in that the capacitor C_2 does not discharge in full and the current in the primary is limited by the resistor R_2 . For this reason, its power is low. The similarity with the circuit in Fig. 4.21 and the observable effect of HF generation in the MHz range with very low power consumption leads to a conclusion that a small HRM effect is taking place. A very good efficiency was obtained by generating a high voltage up to 25 kV AC with low output current on the order of 100 μ A. This was obtained with the following circuit parameters: SG air gap 0.3 mm; HV = 3250 VAC at $C_1 = 8.33 \mu\text{F}$; $C_2 = 1 \text{ nF}$; $R_2 = 2.2 \text{ Mohm}$; $d = 8 \text{ mm}$. According to the Paschen law curve, the breakdown voltage at $d = 8 \text{ mm}$ is 23 kV. PS is a commercial DC HV power supply for a photomultiplier (Venus Scientific Inc., model K30). It is supplied by 15 VDC, current 250 mA. **The total power consumption of this Tesla coil including the HV PS is 3.75 W.**

Fig. 7.11 shows the Tesla coil built with the circuit of Fig. 7.10.

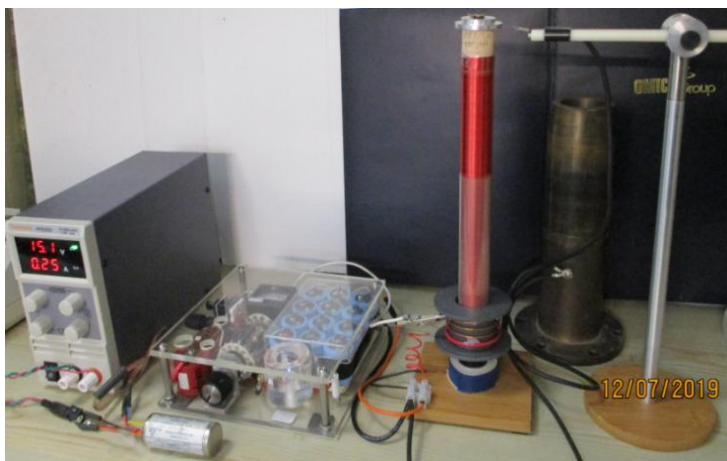


Fig. 7.11. Low power consumption Tesla coil.

The metal cylinder behind the Tesla coil in Fig. 7.11 serves as a ground. The SG and HV (23 kV) sparks are shown zoomed at the bottom of the figure. This Tesla coil delivers an AC output voltage of 23 kV (current about 100 uA) for an input power of 3.75 watts. With such small power consumption, this RF source could work in a continuous mode of operation. The electrodes of SG must be of tungsten with a possibility for precise gap adjustment. One additional important requirement for stable operation is that the circuit needs a connection to a metal object of mass M for stable operation. However, it does not need to be the Earth ground. A metal object with weight no less than 0.5 kg is sufficient. The metal body of the plasma ignition device would meet this requirement.

If the low power consumption Tesla coil does not have enough power for pre-ionization, a more powerful option could be used based on the circuit diagram shown in Fig. 7.3 and the HV AC supply module (Tesla coil driver) shown in Fig. 7.4.

For the pre-ionization purpose, the working chamber with the electrode system shown in Fig. 7.2 must be modified by adding four additional electrodes preferably made of tungsten. They must be isolated from the body and inserted between the other 4 electrodes, but at different heights in order to not affect the path of the HV spark that triggers the plasma explosion. All of them could be connected to the top terminal of the Tesla coil, while the bottom of the secondary should be connected to the metal body. These electrodes should have sharp edges to facilitate the corona discharge between them and the metal body.

7.3.3. Vacuum/gas filling system

We will not describe the preparation of the noble gas mixture. Purchasing of a bottle of Penning type of noble gas mixture is discussed by Bob Rohner in his demonstrations (at 8:00 min) at the Extraordinary Technology conference, 2013 [58]. Before filling with the noble gas mixture, the air of the plasma device must be evacuated. Fig. 7.12 shows schematically the gas-filling system.

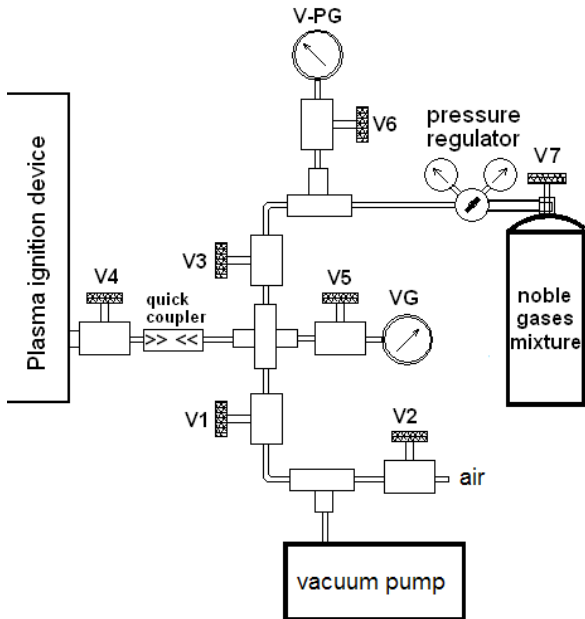


Fig. 7.12. Vacuum/gas filling system

For air evacuation and purging, a one stage oil vacuum pump could be used. In our recent test, a 1/3 HP NORMAN vacuum pump Model RS-1.5 was used. It is specified at 30 Pa, but in the test a minimum of 6 millibars was obtained. The vacuum\pressure gauge VPG2 and the valve V6 are optional if a more precise pressure measurement is desired.

The test procedure is the following:

Open valves V1 and V4 while all other valves are kept closed. Turn ON the vacuum pump until the pressure measured by the vacuum gauge VG drops to about 6-8 millibars. Keep ON long enough for purging (2-4 min depending on purging volume). Then close V1 and open V2 right away (to avoid sucking the oil of the vacuum pump into the connection pipes). Close V5, open V7, and adjust the pressure regulator to about 1 atmosphere, then open the optional valve V6. Open valve V3 slowly and observe the pressure on V-PG to be a little over 1 atmosphere. If without the optional V-PG and V6, watch the piston until it begins to move from the bottom dead position and close the valve V3. Then close valve V4 and

disconnect the vacuum filling system from the quick coupler. The plasma ignition device is ready for test.

7.3.4. Block diagram of the complete test system.

Fig. 7.13 shows the block diagram of the test system. The measurement cylinder is the air cylinder with a piston. The cylinder is filled with air by the air compressor at the desired air pressure. This is discussed in §7.4.2. The modules in the block diagram are the following; TC (Tesla coil) driver shown in Fig. 7.4 with interconnections shown in Fig. 7.3; capacitive charger shown in Fig. 7.5; vacuum/gas filling system shown in Fig. 7.12.

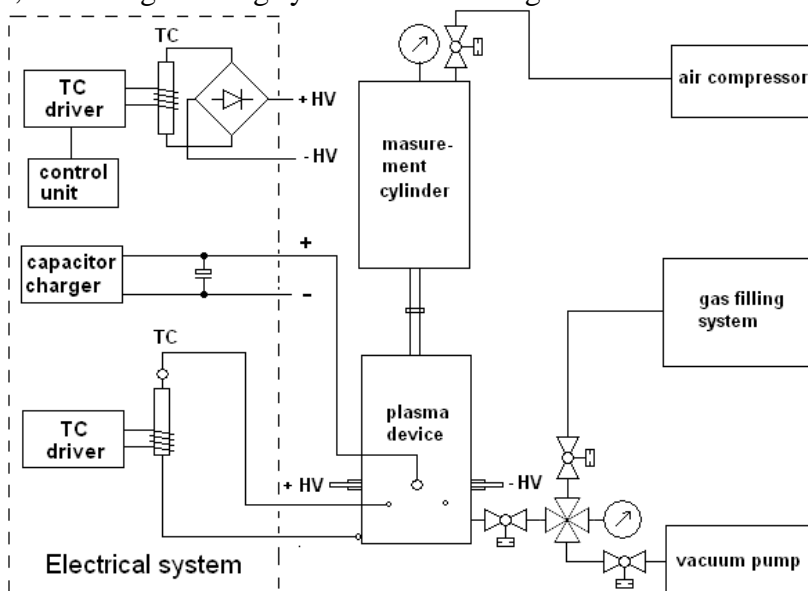


Fig. 7.13. Block diagram of the test system

7.3.5. Calculation of distances between HV electrodes.

The distance between the HV electrodes can be calculated on the basis of breakdown voltage. The direct voltage measurement in the kV range is difficult but it could be calculated with some approximations. For calculation of the breakdown voltage, one may use the Paschen-Townsend formula [86]

$$V_B = \frac{Bpd}{C + \ln(pd)} \text{ [V]} \quad (7.1)$$

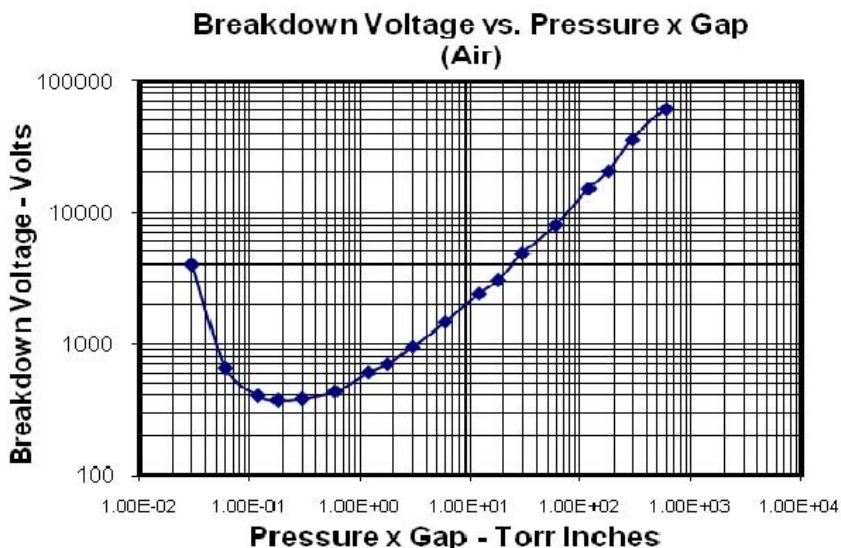
where: $C = \ln(A/\ln(1+1/\Gamma))$, p – pressure (Torr), d – gap (cm)

For air: $A = 15 \text{ (cm}^{-1} \text{ Torr}^{-1}\text{)}$; $B = 365 \text{ (V cm}^{-1} \text{ Torr}^{-1}\text{)}$;
 $\Gamma = 10^{-2}$, then $C = 1.18$

Then the breakdown voltage at normal air pressure is:

$$V_B = \frac{277400d}{1.18 + \ln(760d)} \quad (7.2)$$

For a faster estimate at pressures different from the atmospheric pressure, the monogram of Paschen law shown in Fig. 7.14. could be used.



7.14. Paschen law for estimation of the breakdown voltage

7.4 Energy measuring system and test procedure

7.4.1. Measuring of the input energy:

The input energy for a single plasma expansion is estimated from the values measured by the voltmeters and ammeters. They are preferably of an electromagnetic system, because the scalar (longitudinal) waves generated by the plasma discharge penetrate easily through the common ground line and could damage the digital measurement devices. For a similar reason, the electrical part of the

plasma device must be supplied by batteries in order to be completely separate from the power lines.

The energy for the HV spark is estimated by taking the product of the input voltage, current, and time duration.

The energy of the charged low voltage capacitor spent per single ignition is given by the Eq. (7.3), where U_1 - is the initial voltage and U_2 – is the voltage after the capacitor discharge.

$$E_C = 0.5C(U_1^2 - U_2^2) \quad [J] \quad (7.3)$$

7.4.2. Measuring of output kinetic pulse energy:

The measuring system shown in Fig. 7.13 permits estimation of the output kinetic energy from a single stroke of the gas expansion.

There are two methods of measurement, both used by Bob Rohner. Although only the energy of the expansion phase is measured, the methods are practically useful.

First method: In this method, the measurement system shown in Fig. 7.2 is a weight fixed on the top of the upper rod connected to the piston. The rod slides in a linear bearing fixed to the foundation to which the device is attached. The piston is at the initial bottom position before triggering of the gas expansion, and the sliding rubber O-ring is also in its initial position. After the plasma expansion from a single shot, the O-ring appears displaced to a distance s from its initial position. The estimated pulse energy from the plasma expansion is equal to the work done against the earth gravity acceleration g . It is given by the expression

$$E = (m_1 + m_2)gs \quad [J] \quad (7.4)$$

Where: m_1 is the mass of the piston with rods and load holder [kg], m_2 is the mass of load, s is the O-ring displacement [m], and $g = 9.81 \text{ (m/s)}^2$ is the gravitational acceleration.

In fact, only the output energy from the plasma expansion is measured. There is also energy from the plasma contraction that cannot be estimated by this simple test. However, it is much smaller. If a ratio of input to output energy is obtained that is greater than 100% (physical overunity), the test will definitely be useful.

Second method: In this method, the measuring system shown in Fig. 7.2 is an air pressure cylinder with a piston. The sketch of this air pressure cylinder is shown in Fig. 7.15.

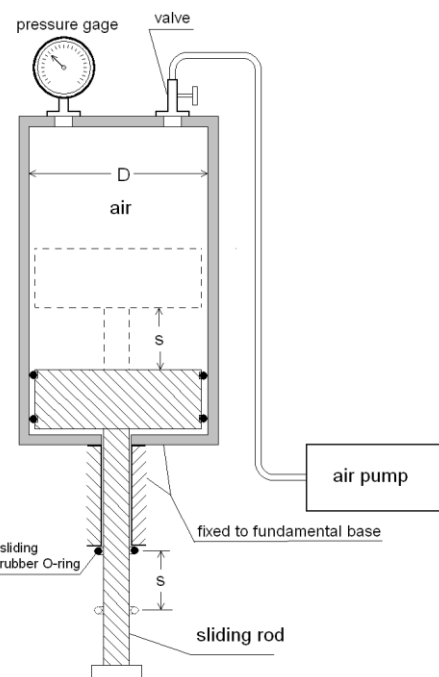


Fig. 7.15. Air pressure cylinder for estimation of the output energy from a single stroke expansion.

The bottom part of the sliding rod touches the rod of the piston in the plasma chamber, while the upper part is connected to the piston of the air cylinder. The efficiency might also depend on the initial working pressure of the noble gas

mixture. With this method, the efficiency could be tested not only for the case of an noble gas mixture at normal atmospheric pressure, but also at greater pressures. This of course will require adjustment of the triggering high voltage and the initial voltage of the capacitor bank. For a test with an noble gas at a pressure above atmospheric pressure, the pressure of the air cylinder must also be the same.

There are two calculation methods in this option for measurement:

Calculation method A: If the volume of the air pressure cylinder is greater than the volume of the noble gas mixture, one may consider that the air pressure is approximately constant at the lower and upper piston positions. The method is more accurate if the expansion force is large. For a small expansion force, the pressure in the air cylinder is close to atmospheric pressure and the estimate is not accurate. The output energy E from a single stroke expansion is estimated as the mechanical work W of a force F for the path s .

$$E = W = Fs \quad [J] \quad (7.5)$$

Under the assumption that the pressure is constant (due to the large volume), the force F is also constant. Then it is calculated by the expression

$$F = AP = 0.25\pi D^2 P \quad [N] \quad (7.6)$$

P is the pressure displayed by the pressure gauge and A is the surface area of the piston with diameter D (internal diameter of the cylinder). Note that the pressure gauge usually measures the differential with respect to the atmospheric pressure. Therefore, the single stroke energy is

$$E = 0.25\pi D^2 Ps \quad [J] \quad (7.7)$$

It is better to use SI units of measurements: P [N/m²], D [m], s [m]. In this case, the physical efficiency is directly obtained as the ratio between output and input energy.

Calculation method B: The measurement in this method of calculation is based on classical thermodynamics. The change of air pressure in the measurement cylinder is taken into account. With some approximations, the process of a single shot could be considered as isothermal and we may apply the ideal gas law. Then the work (energy) is given by the formula

$$E = W = nRT \ln(V_B/V_A) \quad [J] \quad (7.8)$$

Where: V_A – initial volume before expansion, V_B – shrunk volume due to expansion, R – universal gas constant, T - environment temperature in Kelvin, n - number of air moles in the volume. In the system of SI units, we have

$$R = 8.3143 \left[\frac{J}{mol K} \right] \quad - \text{Universal gas constant} \quad (7.9)$$

$$N_A = 6.022 \times 10^{23} \quad - \text{Avogadro number} \quad (7.10)$$

The average number of air molecules in 1 cubic meter at sea level according to a NASA source is 2.5×10^{25} molecules [84]. Dividing by the Avogadro number, one obtains 41.51 moles. The number of moles n in Eq. (7,8) should be $41.51 \times V_A$, where V_A is in [m^3]. This number also depends on the atmospheric pressure at a particular height (elevation). This is easily obtainable if the elevation above the sea level is known.

7.5. Example of energy efficiency estimation using the data published by Bob Rohner for his Plasma Blaster device

In the following example, the test data from Bob Rohner's Plasma Blaster are used. The data are publicly available from his conference talks, interviews and videoclips. The author also contacted him by phone but he intends to keep some know-how in confidence with his team of collaborators. For this reason, some missing data were inferred from a test of similar electrical modules performed by the author and his technical assistant, Velin Asenov.

7.5.1. Input energy for a single plasma expansion pulse

Capacitor value: 4000 microfarads.

Charge voltage: 120 VDC (approximately)

Discharge voltage: 60 VDC (approximately)

The discharge energy was calculated according to Eq. (7.3): **E= 21.6 joules**

The energy for the high voltage spark is not given. (It was obtained from the electrical device built by the author and tested with a spark of 40 kV and duration of 80 μ s. The input energy is 6 joules).

The heavy solenoid coil over the working cylinder of the Plasma Blaster is supplied by 24 VDC with a current about 2 – 3 Amps (according to one of Bob Rohner's interviews). However, it may be applied for only a short time during triggering. If it is ON for 0.1 sec per single triggering, the supplied energy will be 4.8 – 7.2 joules. There will be some losses in the ON-OFF mode from an eddy (Foucault) current in the cylinder and piston, but this could be minimized by a proper design.

7.5.2. Output energy from the single plasma expansion pulse.

Calculation of the output energy from a single gas expansion using the data published by Bob Rohner:

a. By calculation method A: Input data for the air cylinder: D = 2" (5.8 cm), displacement s = 1.75" = 4.44 cm, internal cylinder height of the piston on the bottom is approximately 4.5 " = 11.43 cm, working pressure is 120 psi = 827.37 kPa. (The pressure gauge measures the differential with respect to atmospheric pressure.) The force F according to (7.6) is 1.677×10^3 (N). Then the estimated output energy from a single stroke of plasma expansion, according to Eq. (7.7), is

$$\mathbf{E = 74.54 \text{ (J).}} \quad (7.11)$$

b. By calculation method B: In a single stroke measurement, the gas temperature in the air cylinder is considered unchanged because of the short time of the plasma expansion, so we may use the room temperature of T = 295 (K). The air cylinder volume at the bottom position of the piston (estimated from a videoclip) is 14.137 cubic inches = 1.954×10^{-4} (m^3). The change of volume for a single expansion is $V_A/V_B = 1.636$. Pressure gauges usually measure the differential with respect to atmospheric pressure. The absolute pressure is needed for an accurate number of air moles in system SI units, so the absolute atmospheric pressure should be added to the differentially measured pressure. Then the initial pressure is 120 psi + 14.7 psi = 134.7 psi. The corrected number of moles in one cubic meter at this pressure is $41.51 \times (134.7 / 14.7) = 380.4$. The working volume V_A in m^3 is 1.954×10^{-4} (m^3), so the number of air moles is 0.074. An additional small correction is needed because of the air pressure dependence on elevation. Bob Rohner performed the test at the elevation of 206 m where the air pressure is 98874.6 (Pa). At sea level it is 101325 (Pa), so the correction factor for number of moles is 0.976. Then the involved number of air moles calculated for the working pressure of 827.37 kPa, corrected for the local elevation, is 0.072 (moles). Putting all data in (7.8), we obtain the value of the output energy from a single stroke of plasma gas expansion:

$$\mathbf{E = 89.8 \text{ [J]}} \quad (7.12)$$

We consider that the calculation method B is more accurate. In method A the air pressure is slightly increased during the plasma expansion and this makes the piston displacement s smaller. We do not have all necessary input data for Bob Rohner's Plasma Blaster, for example, the HV spark energy and RF source energy. So we had to make calculations based on the test data from our input modules. Table 7.1 shows the energy balance from a single expansion phase. X_1 and X_2 are the data missing from the Bob Rohner Plasma Blaster tests.

Table: 7.1. Energy balance for a single gas expansion

	HV spark	Capacitor	RF source	Solenoid 0.1 s ON	Total [J]
Input energy	X_1	21.6 [J]	X_2	7.2 [J]	28.8+ X_1+X_2
Output energy					89.8 [J]

For 100% efficiency, the input energy of the HV spark and RF source (X_1+X_2) must be smaller than 60 joules. From the author's test results, the energy X_1 could be optimized to 8 joules per stroke if the HV spark source is properly designed. The minimization of X_2 energy could be achieved if a properly designed Tesla coil is used for the RF source. The power consumption by the solenoid also could be eliminated by using permanent magnets, as shown in Fig. 7.2.

- **The conclusion is that in a properly designed plasma ignition device with optimized input sources and a proper noble gas mixture, it is possible to achieve physical overunity.**

Presently, a more confident analysis of Bob Rohner's Plasma Blaster is not possible due to the lack of some data. Bob also claims that he observed an electrical pulse between anode and cathode from the plasma collapse, and he considers it to be part of the output energy. He takes the pulse through a diode and charges a capacitor. The author tried to detect such a pulse which must have a polarity opposite to the capacitor discharge. However, it was found that the diode rectifies an RF emission from the triggering HV spark. If Bob

Rohner uses an RF generator (he mentioned it at 26 MHz), the energy of the pulse he detects could also come from this source. If this is the case, the pulse cannot be considered to be a useful output.

7.6. Conclusions and technical recommendations for researchers.

The author recommends using the principle of Papp's engine instead of the Testatika principle. The latter is not only difficult to build, but also more vulnerable to external environmental conditions. From the analysis of the patents in Chapter 4, the published data of experimenters, as well as the author's experimental work, we arrive at the following conclusions and technical recommendations.

Conclusions:

1. The physical process in Papp's engine has a signature in common with natural lightning (thunderstorms). In both cases, a Heterodyne Resonance Mechanism (HRM) takes place. The energy from the physical vacuum is accessed by clusters of oscillating ion-electron pairs. The energy stored in these clusters is released in an avalanche process triggered by a strong current. The magnetic field of this current destroys the clusters of ion-electron pairs. The accumulated energy is conveyed to the ions (some of them recombine to neutral molecules) causing a gas expansion.
2. The application of an axially oriented magnetic field from a solenoid (or permanent magnet) in Papp's engine and the Plasma Blaster helps to align the clusters. Therefore, the released energetic ions (or neutral molecules) following the avalanche process will be predominantly in the direction of the piston motion. For this reason, the increase of the temperature of the working cylinder (chamber) is insignificant in comparison to the gas combustion engine. This is not a classical thermodynamic effect. Dr. McKubre, who has been in contact with Bob Rohner, expressed a similar idea based on extensive tests.
3. The use of a mixture of noble gases is more effective. They do not enter into chemical reactions and their ionization (only single

ionized atoms) directly leads to formation of ion-electron pairs. Negative ions cannot work but their number is insignificant.

4. The energy efficiency (input/output) depends on the quantity of ion-electron pairs. It can be increased by using properly selected radioactive isotopes (those that are known to create Rydberg matter).
5. A radiofrequency source could also be helpful in the formation of ion-electron pairs because it stimulates the HRM frequency in the MHz range (see HRM RF spectra in §4.5.3).

Technical recommendations:

1. The author recommends building a plasma ignition device with a magnetic field from permanent magnets according to the sketch in Fig. 7.2.
2. For the electrical system, the suggestion is to use the electrical block diagram shown in Fig. 7.3, the circuit diagrams for HC AC module in Fig. 7.4, the capacitor charge module built as per the circuit shown in Fig. 7.5. and a Tesla coil built according to the circuit shown in Fig. 7.10.
3. For optimization of the energy efficiency by estimation of the output energy, the recommendation is to use initially the first method of §7.4.2 (with a weight on the top) and then the second method (with an air pressure measurement cylinder).
4. The second method of §7.4.2 permits experimenting at different initial pressures of the measuring air cylinder. The energy efficiency may depend on the initial pressure of the noble gas mixture.

7.7. Considerations for technical overunity

7.7.1 Kinetic to electrical energy conversion

Obtaining physical overunity is necessary but not a sufficient requirement for achieving technical overunity. Additionally, the use of the Papp engine principle is accompanied by the following problems:

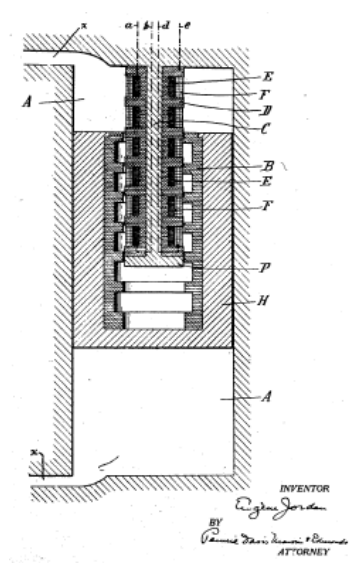
- 1. Significant difference between expansion and contraction times (fast expansion and slow contraction)**

- 2. Time jittering in consecutive triggerings**
- 3. Missing or not-triggered strokes**

In the combustible gas engine, the first problem does not exist, while problems 2 and 3 are enhanced for sufficiently high RPMs. In Papp's principle, the expansion and contraction phases are both workable, but with quite different time durations. The above-listed problems make it difficult to use the plasma ignition principle in a classical rotation device with one or more cylinders. It is especially difficult for higher RPMs. These problems have been a serious obstacle for Papp prototypes and possibly caused a tragic incident during one of his demonstrations. They have been serious obstacles for other experimenters. A different technical solution was investigated by Bob Rohner, for example, by using a rotating turbine. However, this option has other problems that interfere with obtaining overunity.

The most promising choice is a single cylinder plasma ignition device with a piston connected to a **linear generator** (alternator). It will have the following advantages.

- **The problem of the time difference between the expansion and contraction phase is eliminated**
- **It will permit conversion of input to output electrical energy.**



One of the earlier patents about a linear generator is the "generator of electrical current" by E. Jordan, US patent 1,544,010 (April 24, 1923). It converts the kinetic energy of reciprocated motion into electrical current. The device is illustrated in Fig 7.16.

Linear generators today have practical applications and their design is optimized for higher efficiency. F. Rinderknecht and Hans-George Herzog show optimization of a linear generator for a hybrid vehicle [90]. In another article, Sandra Eriksson from

Uppsala University, Sweden, describes a simulation model for the design of a permanent-magnet linear generator [91]. The model shows that an efficiency of 85% could be achieved with an output power of 18 kW.

It is evident that the linear generator must be customized to obtain the maximum possible efficiency of the kinetic to electrical conversion.

7.7.2 Estimation of necessary efficiency of the Plasma device for obtaining net output energy (power).

The step to build a device or engine_with technical overunity is not justified unless a minimum physical overunity is obtained. The test of the plasma ignition device illustrated in Fig. 7.13 gives this possibility. Although only the energy of the expansion phase is measured, the approximate estimate is useful.

It is evident that the physical overunity estimated for a single stroke must be greater than 100% in order to compensate for losses in the conversion of kinetic to electrical energy. Additionally, the electrical output must supply the energy required by the input modules. This involves also the efficiency of a necessary voltage converter. On the other hand, a level of pre-ionisation of the noble gas mixture is needed for the device to work continuously in consecutive triggerings. For this purpose, it is more convenient to consider power technical overunity instead of energy overunity. In such case, we must consider the number of triggerings, N per second. The expected useful net electrical power P_{net} can be estimated by the equation

$$P_{net} = E_{out-pulse} \eta_{k-e} N - P_{inp} \eta_{V-conv} \quad (\text{W}) \quad (7.13)$$

where: $E_{out-pulse}$ - is the output energy of a single expansion/contraction phase, η_{k-e} is the efficiency of the kinetic to electrical energy conversion by the linear electrical generator, N is the number of ignitions, P_{inp} is the required input power, and η_{V-conv} is the power efficiency of the output to input voltage converter.

From the web page of Bob Rohner (rgenergy.com) we see that he demonstrates 3 or 4 consecutive firings (triggerings) per second. Let us consider N=3. The input power of the capacitive charger will depend on N. Using the estimated capacitance energy per one stroke of 21.6 joules (§7.5.1) (let us accept 22 joules), for N = 3 we will have 66 (W). If the power efficiency of an optimized capacitor charger is 75%, the power consumption of the capacitor charger will be 88 (W). The power of the input RF generator used by Bob Rohner is unknown. Instead of that, we may use the power of the low consumption Tesla coil presented in Fig. 10 and 7.12. The measured input power was 3.75 W. We will use 5 W but with reservations. In our plasma device, we will use the permanent magnet in the working chamber instead of the external solenoid. For conversion of kinetic to electrical energy, we will consider a linear generator. For this purpose, an optimized linear generator is necessary. The efficiency of such a generator could be up to 85%, according to [90,91], but we will use a conservative value of 60% due to the significant time difference between the expansion and contraction phases. From a number of observations, we can accept that the time of the contraction phase is about 5 times longer. This means that the kinetic energy from this phase will be 5 times smaller.

Table 7.2 shows the power breakdown budget from all input electrical devices and output electrical power from the linear generator connected to the plasma ignition device. We used some data from the Bob Rohner Plasma Blaster, and data that were missing we obtained from our experiments and observations. For example, the power of the HV AC module is 27 W in continuous mode. If a single triggering needs a HV spark operation of 100 ms, the energy for a single triggering is 2.7 (J). The power consumption of a pre-ionizing Tesla coil working in continuous mode is accepted to be no larger than 8 (W). The output kinetic pulse from a single expansion is accepted as 90 (J) (Eq. 7.12).

Table: 7.2. Electrical energy balance for a Plasma ignition device with a linear electrical generator

Power of input modules				Total Input power [W]	Kinetic to electrical efficiency $\eta = 60\%$				Power Over-unity
	E [J]	N #	Power [W]		E _{exp} [J]	E _{con} [J]	N #	Power [W]	
HV AC module	2.7	3	8.1						
		4	10.8						
		5	13.5						
Ionizing Tesla Coil			8						
Capacitor charger $\eta = 75\%$	22	3	88	104.1	90	18	3	194.4	186
		4	117.3	128.1			4	259.2	202
		5	146.6	160.1			5	324	202

Where: $E [J]$ – input pulse energy, N – number of pulses, $E_{exp} [J]$ – plasma expansion stroke energy, $E_{con} [J]$ – plasma contraction stroke energy

Assuming that the contraction time is 5 times slower, the kinetic pulse energy from contraction will be 18 [J]. The efficiency of the linear generator is considered to be 60%. That is conservative in comparison to the theoretically optimized value of 85% for kinetic to electrical conversion [91,92].

According to one certificate of the original Papp engine test [94], it was run at 726 RPM which corresponds to 12 strokes per second. From Table 7.2 we see that the electrical power overunity does not depend strongly on the triggering rate because the major fraction of input energy belongs to the capacitor charger. Let us consider 4 triggerings per second with an output power of 259.2 W, for which the power overunity is 202 %. For a closed system, a fraction of this power must supply the input modules. In order to minimize the heat loss in the capacitor charger, it should have a short transient time in its on-off mode. It must be supplied by a battery, because the initial charge current is large. The most suitable source is a 12 VDC lead acid battery. For a capacitor charger with an efficiency of 75%, the

needed power for 4 strokes is 117.3 W. The total input power including the HV AC module is 128.1 W. Assuming that the power converter from output to input voltage has an efficiency of 80%, the fraction of the output power needed to keep the battery charged will be $128.1/0.8=160.1$ W.

**Then the net electrical output from the given overunity is:
259.2 – 160.1 = 99.1 (W).**

We see that the overunity in the above case depends strongly on the efficiency of the kinetic to electrical converter. We used a quite conservative efficiency of 60% for the linear generator.

We use a very conservative approach in calculation of the net electrical output in Table 7.2. It was observed that at the start, the minimum low voltage needed for the plasma ignition is higher than for the consecutive triggerings. In our test, the plasma ignition for example began at 340 V (capacitor of 800 uF charge) and the capacitor was discharged to 70 V. In the following triggerings, the plasma ignition began at 310 V and the capacitor discharged to 90 V. A similar but much stronger effect is observed by Bob Rohner in his device. He even initially activated the high voltage spark a few times without discharging the low voltage capacitor. Then the plasma ignition worked at a lower voltage of the charge capacitor. In other words, the output pulse energy in this case is the same, while the input energy for the consecutive plasma ignitions decreases with respect to the initial ignition. The conclusion is that a pre-ionized condition of the noble gas mixture is important. This corresponds to some necessary quantity of ion-electron pairs.

- **Some necessary quantity of ion-electron pairs must exist prior to triggering of the plasma ignition.**

In the Joseph Papp engine and the Plasma Blaster of Bob Rohner, the radioactive source enclosed in the two buckets (anode and cathode) and the RF generator partly satisfy the above-mentioned requirement. (Bob Rohner used different radioactive isotopes). However, some improvement could be made. For generation of ion-electron pairs (Rydberg matter), the most suitable elements are radioactive isotopes that emit positive Beta particles. However, their abundance is very low and one must use artificially obtained isotopes. A suitable choice is ^{66}Ni that emits positive beta Beta particles and decays to a stable isotope ^{66}Cu .

Another improvement over the Joseph Papp and Bob Rohner devices is to use a multiple frequency emitter in the RF range instead of a single frequency emitter. Different noble gases could be ionized by different frequencies. The use of a Tesla coil with a spark gap is the preferred choice. It generates scalar waves in a broad frequency range that covers the HRM frequency band. According to BSM-SG, the magnitude of the scalar waves attenuates faster with distance than the EM waves, but at close distances they are more effective for ionization. For this purpose, the Tesla coil described in §7.3.2 could be used.

From a theoretical and practical viewpoint, the physical overunity would also be improved if the volume of the working chamber is larger. In Bob Rohner's Plasma Blaster, the internal cylinder diameter is about 2". Better results could be achieved with a 3" or 4" diameter. This would also require bigger values for the high voltage (for the spark) and for the voltage of the capacitor.

In our case, the kinetic energy difference between the expansion and contraction phases will decrease that efficiency by a few percent, but computer models for optimization already exist. The example of the calculations in Table 7.2 suggests that a minimal physical overunity must be achieved in order to obtain an electrical net power. If this goal is reached, the next step is a selection of kinetic to electrical energy converter. Keeping in mind the problems 1, 2 and 3 in §7.7.1., the preferred converter is a linear electrical generator based on the principle shown in Fig. 7.16.

Presently, advanced designs of linear generators exist for hydrogen cells and hybrid vehicles [90,91]. The article of Sandra Eriksson (Uppsala University) about the design of a permanent magnet linear generator shows that a theoretical efficiency of 85% could be achieved [91].

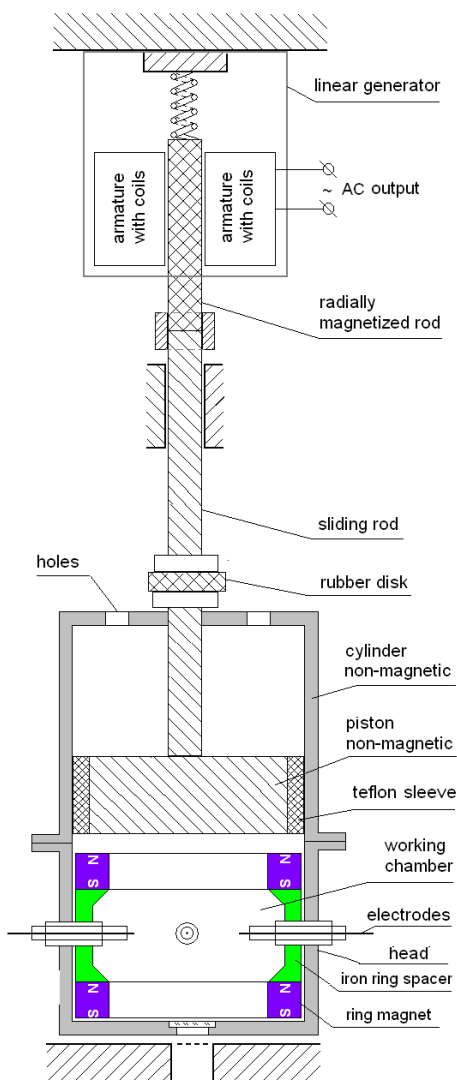


Fig. 7.17.

Conclusions and considerations:

1. The net output electrical power of 99.1 (W) is a conservative estimate if using a linear generator with efficiency of 60% (Table 7.2).

Fig. 7.17 shows the connection of the plasma ignition device with a linear generator. The sliding rod of the piston is connected to a radially magnetized rod that moves inside of the stator armature of a linear generator. The latter is stationary and contains coils in which current is generated when the magnetized rod is moving. The AC output should be conveyed to a bridge rectifier.

2. In prolonged operation, the quantity of the noble gas mixture could eventually leak out.

The problem 2. could be solved if the noble gas mixture is sealed hermetically. One of the Papp engine experimenters, Heinz Klostermann, suggested a sealed twin device with two explosion (working) chambers [95]. The main disadvantages of such a solution are two: (1) it is quite difficult to obtain properly synchronized plasma explosions in the two working chambers and (2) the orientation of ion-electron clusters does not provide an efficient unidirectional push to both pistons as discussed in the next section.

7.7.3. Twin piston device with linear generators

Fig. 7.18. shows a technical solution to the problem 2 (of §7.7.2) consisting of a twin piston plasma device with a common working chamber and two linear generators.

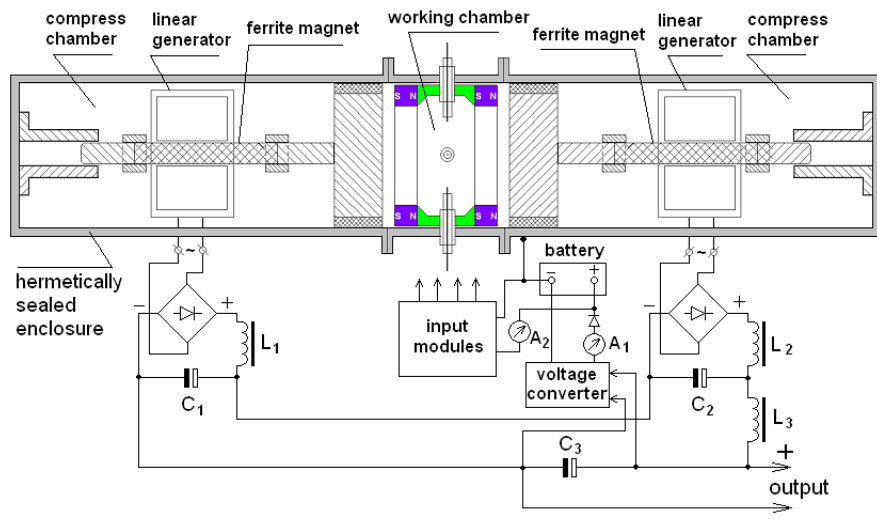


Fig. 7.18. Twin piston plasma device with two linear generators.

The device contains a common working chamber and two compression chambers. The two pistons have sealing sleeves preferably from Teflon. The plasma ignition causes pistons motions in opposite directions. The working and compress chambers have

separate valves for the noble gas filling. The gas pressure in working and compress chambers must be equal. The gas in the two pressure chambers will not be ignited and will serve as springs. Some small fraction of the output energy will contribute to heating the compressed chambers and this must be taken into account. Depending on the design of the linear generators, their coils may provide an output AC voltage with a frequency equal to the ignition rate or with a higher AC frequency. In the first case, the chokes L_1 , L_2 , and L_3 must be low frequency. Such chokes are quite heavy. If the linear coils are specially designed to give a higher frequency output, the chokes could be much lighter. The voltage converter is needed because the output voltage could have a different value which will vary with the plasma ignition rate. The efficiency of the converter should be taken into account for charging the battery. The integral current measured by the ammeter A_1 must be positive and greater than the current measured by A_2 . This will serve as an indication that we have electrical overunity.

The twin plasma device is expected to have a few additional advantages over the one piston device shown in Fig. 7.15. One of them is apparent from a theoretical aspect.

Let us denote the cylindrical axis by X. The magnetic field in the working chamber helps to orient the ion-electron superclusters along the X axis. However, the electron trajectories in some of them could be clockwise and in others it could be counterclockwise. Therefore, some of the released ions after the destruction of the ion-electron pairs will have a momentum in the +X direction and others in the -X direction. Then both of them will exercise a unidirectional pressure on the pistons. In the case of a single chamber with one piston, only half of the released ions will exercise direct pressure on the piston. The other half will exercise a pressure on the wall. Only then will it contribute to the piston motion similar to a backscattering reflection, but this type of reflection is not unidirectional. For this reason, the efficiency of the twin plasma ignition device will be greater than the efficiency of the single piston device.

The other advantage is that the gas in the two compressed chambers will serve as springs. After the plasma expansion, the two pistons will tend to return to their initial position. This will shorten

the time of the contraction phase, which will reflect a greater efficiency of the linear generator. The gas compression in the compression chambers is a thermodynamic process that will contribute to some heat, but the tradeoff is expected to be in favor of the linear generator's efficiency.

The idea of twin axially aligned cylinders with two linear generator pistons and a common working chamber is not new. Etagen Technology offers a similar device, but their design is for a combustion device using natural gas fuels, biofuel, or hydrogen [96]. Presently, a number of companies offer efficient linear electrical generators to be used in hybrid vehicles. Computer models also exist for optimizing the efficiency of such generators. According to the model of Sandra Eriksson from Uppsala University, an efficiency of 87% could be achieved for a linear generator with a fixed or a variable pole pitch [91]. The company LG built a linear compressor for refrigerators [97]. It contains the same functional blocks as the linear generator and could be redesigned.

7.8. Summary and general conclusions

The theoretical and experimental research shows that a properly designed device for accessing zero point energy, ZPE-D, is feasible, but the net energy output is not unlimited.

7.8.1. Volumetric energy density of the ZPE-D accessible by the HRM effect.

The volumetric energy density was theoretically discussed at the end of Chapter 1, and Appendix A of the paperback version. Its measurement unit in SI system is the energy in joules per unit cubic meter [J/m^3].

The volumetric energy density of ZPE-D is thousand times smaller than the volumetric density of the ZPE-S energy that is directly connected to the nuclear energy obtained by nuclear fusion or fission reactions. The most important difference is the flowing:

The nuclear energy obtained by accessing the ZPE-S by nuclear fusion or fission reactions involves a change of the CL

microcurvature around the superdense nucleus, which means a small change of the CL internode distance. The superstrong SG energy is released as mass change estimated by the Einstein equation $E = mc^2$. This is enormous energy. From the other hand the vibrational type of ZPE-D energy is distributed uniformly in space, but the access to it HRM effect does not cause disturbance of the average distance between the CL nodes, therefore no nuclear transmutations could take place. Only the internal energy of the electron is affected, but it is restored during the quantum mechanical interactions of the electrons with the CL node oscillations. Therefore the amount of the zeropoint energy that could be accessed by the HRM effect will be much smaller in comparison with the nuclear energy obtained in the nuclear plants.

The smaller volumetric energy density of the ZPE-D means that extracted energy depends on the volume in which the HRM effect is involved. For example in the case of lightning phenomenon the volume in which the HRM effect takes place is enormous, while in experiments it is comparatively very small.

There are also some other obstacles that may need additional research on this new energy.

- **The Heterodyne Resonance Mechanism (HRM) predicted in BSM-SG unified theory permits both: (1) a local gravity control [18] and (2) access to the zero point energy of the physical vacuum.**
- **The spectral signature of the HRM effect is clearly identified in experiments involving glow discharge of neutral plasma**
- **The HRM effect involves properly activated, oscillating ion-electron pairs in which the electrons interact with the physical vacuum at the superhigh Compton frequency.**
- **During specific synchronized oscillations, the electrons take a fraction of zero point energy.**
- **The HRM effect is identified in natural lightning phenomenon.**

- In the avalanche process of creation and destruction of ion-electron pairs, the accessed zero point energy is released as a pressure pulse
- In a properly designed plasma ignition device, the pressure pulse provides kinetic energy in which a non-thermodynamic process takes place
- A twin piston plasma device is most promising for obtaining a net output electrical energy (power).
- The amount of the net output electrical energy will be increased with the ignition rate number and the working volume.

The understandable connection between the physics of the HRM effect and its technical realization permits optimization of the plasma device for obtaining physical and technical overunity. Some problems like the lower volumetric energy density (in comparison with nuclear energy), the necessary use of radioactive isotopes and the unknown biological effect will restrict this energy from broader commercial applications. **However, it could be successfully used in space environments, especially for distant space travels.**

The experimental method described in §7.3 provides very useful directions for researchers and experimenters. Instead of following blindly the published so far material as patent applications, videorecords and interviews with experimenters the proposed technical procedures will save a lot of time and money, while leading fast to the stated goal.

It must be mentioned that the energy accessed by the HRM effect could not replace other sources of energy including the nuclear energy from the power plants. The competitive option of the latter is the cold fusion nuclear energy that is completely feasible from a viewpoint of BSM-SG theory [6]. Its main advantage is a minimal or complete lack of radioactive waste.

AUTHOR BIOGRAPHY

Stoyan Sarg - Sargoytchev is a Bulgarian-born Canadian. He holds an engineering diploma and a PhD in physics in the field of space research. From 1976 to 1990, he was involved in satellite and space mission scientific projects sponsored by the international program Intercosmos, coordinated by the former Soviet Union. During this period, he also participated in collaborative programs with India and the European Space Agency. For his pioneering work in space research, Dr. Sargoytchev has been awarded medals from the Bulgarian government and from the Intercosmos organization.

In 1990, Dr. Sargoytchev was invited as a visiting scientist to Cornell University and worked for 1 year and 8 months in the Arecibo Observatory, as P.R. on a Lidar project funded by the NSF (USA). This is the place with the world largest radio telescope or radar. In September 1991 he accepted a position of scientist in Canada and was involved in building a Lidar system at the University of Western Ontario. In 1993 he was employed as a project scientist at the Institute for Space and Terrestrial Science (later CRESTech) working on space projects coordinated by the Canadian Space Agency. Since 2002 he was with York University, Toronto, Canada.

Dr. Sargoytchev worked on diversified projects, obtaining experience in different fields of Space Engineering and Physics. During his 37 years working in academic institutions, he participated in many conferences and seminars. He paid particular attention to unsolved mysteries for which contemporary physics still does not offer an answer. After studying extensively the history of physics, Dr. Sargoytchev realized that the origin of all problems is in the incorrect concept generally adopted about space. Focusing on this issue, he conceived an original idea about space, time and matter that had not been explored before. After a few years of intensive but rewarding work, he developed and published in 2001 his treatise, called Basic Structures of Matter - Supergravitation Unified Theory (BSM-SG). The work was based on a revolutionary new idea that challenges the established view on space, time and matter. The treatise was published under the author's name, Stoyan Sarg. Although he has over 70 scientific publications and some patents in the field of space research, Dr. Stoyan Sarg Sargoytchev considered this theoretical work to be a major achievement in his life. He was convinced that he had found a solution to fundamental problems in Physics in a way that was considered impossible in the past 100 years. He built a successful unified theory in a real 3-

dimensional space which revealed relations between the gravitational, electric and magnetic fields. The monograph “Basic Structures of Matter” has two electronic editions archived in the National Library in Canada (2002) and a few publications in scientific journals. In 2006 he published the whole theory as a book entitled “Basic Structures of Matter – Supergravitation Unified Theory”. A short popular version of his theory was previously published in 2004 as a book titled “Beyond the Visible Universe”. A reviewing committee from the Canadian Association of Physicists published a review of his two books in Physics in Canada Journal vol. 62, No 4, 207-207, (2006).

Amongst the conclusions for potential applications predicted by BSM-SG theory, the most important are the following:

(1) Unveiling of the underlying lattice type structure of the physical vacuum and structures of the elementary particles and atomic nuclei;

(2) A possibility to control the gravitational and inertial mass of a material object;

(3) Unveiling of hidden space energy of non-EM type – a primary source of nuclear energy;

The first conclusion allows understanding of the quantum mechanical interactions between the elementary particles and the physical vacuum. The spatial configuration of atomic nuclei is potentially useful for structural chemistry, nanotechnology and LENR research.

The second conclusion predicts development of a completely new propulsion mechanism suitable for distant space travels. This issue is presented in the book “Field Propulsion by Control of Gravity – Theory and Experiments”.

The third conclusion offers a new vision for two types of hidden energy in physical vacuum: a static type (ZPE-S) and a dynamic type (ZPE-D). The ZPE-S energy appears to be a primary source of the nuclear energy. The book “Structural Physics of Nuclear Fusion” provides theoretical and experimental treatment of this issue. The present book provides theoretical and experimental considerations for accessing the ZPE-D energy.

In 2012, Dr. Stoyan Sarg Sargoytchev was elected as Distinguished Scientific Adviser to the Board of Directors of the World Institute for Scientific Exploration (<http://instituteforscientificexploration.org>).

Articles related to BSM-SG theory are published in peer-reviewed journals, proceedings and physical archives. Some selected scientific and popular articles are available on-line (also by search: Stoyan Sarg)

http://vixra.org/author/stoyan_sarg/

Author's webpage: www.helical-structures.org

OTHER BOOKS BY THE AUTHOR

1. *Beyond the Visible Universe - from a new space-time concept of the physical vacuum* Google book, (2005), ISBN0973051531
2. *Basic Structure of Matter – Supergravitation Unified Theory*, Trafford Publishing, 2006, ISBN 1412083877 (books review in "Physics in Canada,", **62**, No. 4, July/Aug, 2006).
3. *Field Propulsion by Control of Gravity, Theory and Experiments*, ISBN 9781448693085, amazon.com, (2008).
4. *Structural Physics of Nuclear Fusion with BSM-SG atomic models*, ISBN 9781482620030, Amazon.com, (2013)
5. *Пространство Материя Гравитация*, издательство на БАН, София, (2007).



GLOSSARY

Definition of terms used in this book. Some of them are not usually found in scholar physics textbooks.

Basic Structures of Matter – Supergravitation Unified Theory (BSM-SG) is built on an original concept of a space medium that defines the properties of the physical vacuum. It is different from the old concept of the ether as an ideal fluid. A detailed physical model of the space medium is a 3D grid called a **Cosmic Lattice (CL)**, the building sub-elements of which are CL nodes consisting of two types of superdense intrinsic matter. **Supergravitation (SG)** is an energy interaction process between the intrinsic matter objects in empty space. Newtonian gravity is a propagation of the SG field at a far distance by the CL structure. CL nodes are flexible and their properties permit understanding the relation between Newton's gravity and electrical and magnetic fields. The CL structure is distributed everywhere in the visible Universe.

The Supergravitation law (SG) defines the gravitational forces between the CL nodes. It is distinguished from Newton's law of gravity in that the forces are inversely proportional to the cube of distance. SG forces are very strong in proximity to elementary particles and they are behind the strong nuclear forces.

ZPE-S (zero point energy of static type) is a hidden energy contained in the CL space, and is based on the superstrong SG forces. It is the primary source of nuclear energy.

ZPE-D (zero point energy of dynamic type) is a vibrational type of energy. It is a thousand times smaller than the ZPE-S energy but is directly connected to it. It is uniformly distributed in the visible Universe.

Structure of elementary particles: All stable elementary particles consist of helical structures. The building blocks of the structures are identical to the building blocks of the CL nodes, but have a complex spatial configuration maintained by the SG forces.

Structures of the elementary particles and the BSM-SG atomic models are real physical models possessing well defined physical

dimensions. In contrast, the quantum mechanical models are mathematical, working only with energy levels.

SPM (spatial precession momentum) vector is a specific mathematical vector that describes the complex spatial oscillations of the CL nodes. It is involved in the definition of the speed of light according to the BSM-SG physical models.

Space microcurvature: Space curvature around the superdense atomic nucleus is characterized by a small shrinkage of the average distance between the CL nodes. This is similar to the space curvature around a heavier astronomical object predicted by Einstein's General Relativity, but is logically explained by the CL space model.

Ion-electron pair corresponds to the Rydberg state of the atom, but with clearly defined physical properties that distinguish it from the quantum mechanical models of the atom. In experimental observations of neutral plasma, the ion-electron pairs correspond to **Rydberg matter**.

Compton frequency was experimentally discovered by Arthur Compton (1892-1962). In BSM-SG theory, both the electron and the CL nodes possess spatial oscillation features in which the Compton frequency is involved.

Confined electron velocities are the preferred velocities of the moving electron due to the interaction of its oscillations with the oscillating CL nodes.

Quantum orbit is the orbit of an electron having a velocity equal to a confined velocity. When the orbiting electron is near atomic nuclei (proximity field), its energy is defined not only by its velocity, but also includes a fraction of the SG field energy.

Neutral plasma is a plasma of ionized gas or gases containing the same number of electrons and ions while not forming chemical compounds. In our case the gas atoms must be single ionized.

REFERENCES:

1. Michelson, A. A. and Morley, E. W. "On the Relative Motion of the Earth and the Luminiferous Aether." *Philosophy Magazine*. **24**, 449-463, 1887.
2. D. Miller, The Ether-Drift Experiment and the Determination of the Absolute Motion of the earth, Review of Modern Physics, **3**, 203-241, (1933).
3. S. Sarg, New approach for building of unified theory,
<https://arxiv.org/abs/physics/0205052> (May 2002)
4. S. Sarg ©2001, *Basic Structures of Matter*, monograph,
<http://www.nlc-bnc.ca/amicus/index-e.html> (First edition, ISBN 0973051507, 2002; Second edition, ISBN 0973051558, 2005),
(AMICUS No. 27105955), LC Class no.: QC794.6*; Dewey:
530.14/2 21
5. Stoyan Sarg, *Basic Structures of Matter –Supergravitation Unified Theory*, Trafford Publishing, 2006, ISBN 1412083877 (books review in "Physics in Canada," **62**, No. 4, July/Aug, 2006).
6. Stoyan Sarg, *Structural Physics of Nuclear Fusion with BSM-SG atomic models*, ISBN 9781482620030, Amazon.com, (2013)
7. Stoyan Sarg Sargoytchev, Theoretical feasibility of cold fusion according to the BSM atomic models <http://www.journal-of-nuclear-physics.com/?p=864&cpage=10>
8. Stoyan Sarg, Nickel-Hydrogen Cold Fusion by Intermediate Rydberg State of Hydrogen: Selection of the Isotopes for Energy Optimization and Radioactive Waste Minimization, general science Journal, (2014)
<http://gsjournal.net/Science-Journals/Essays/View/5281>
9. Stoyan Sarg, slide shares from conference presentations
<https://www.slideshare.net> (search my name)
10. Stoyan Sarg, selected articles on-line
http://vixra.org/author/stoyan_sarg
11. Barry Setterfield, Exploring the Vacuum, Journal of Theoretics, (2002),
12. S. Sarg, A Physical Model of the Electron according to the Basic Structures of Matter Hypothesis, Physics Essays, vol. **16** No. 2, 180-195, (2003); <https://www.ingentaconnect.com/content/pe/pe>
13. S. Sarg © 2001, *Atlas of Atomic Nuclear Structures*, ISBN 0973051515

HIDDEN SPACE ENERGY

- <http://www.nlc-bnc.ca/amicus/index-e.html> (April, 2002),
(AMICUS No. 27106037); Canadiana: 2002007655X, LC Class:
QC794.6*; Dewey: 530.14/2 21
14. S. Sarg © 2001, Atlas of Atomic Nuclear Structures according to the Basic Structures of Matter Theory, Journal of Theoretics (Extensive papers, March, 2003);
 15. Malcolm Gregor, *The enigmatic electron*, Kluwer Academic Publisher, ISBN 0-7923-1982-6, (1992)
 16. Stoyan Sarg, Gravito-inertial Propulsion Effect Predicted by the BSM – Supergravitation Unified Theory, 26 Annual Meeting of Society for Scientific Exploration, East Lansing, MI, (2007)
 17. Stoyan Sarg Sargoytchev, Method and apparatus for spacecraft propulsion with a field shield protection”, CIPO Canada, patent application 2,638,667, Filing date: August 26, 2008.
 18. Stoyan Sarg, *Field Propulsion by Control of Gravity, Theory and Experiments*, ISBN 9781448693085, amazon.com, (2008).
 19. Wade. L Fite, Production of Negative Ion and Noise in Negative ion Beam, Physical review, **19**, No 2, 411-415, (1953)
 20. P.K. Shukla and B. Eliasson, Physical Review Letters, 108, 165007 (2012)
 21. Stoyan Sarg, The role of the plasma with a heterodyne resonance mechanism in overunity devices,(2010)
<https://peswiki.com/article:the-role-of-the-plasma-with-a-heterodyne-resonance-mechanism-in-overunity-devices>
 22. Stoyan Sarg, Heterodyne resonance mechanism in plasma, youtube videoclip, (2011)
<https://www.youtube.com/watch?v=S0UMkQc4I-U>
 23. Stoyan Sarg, Zero point energy from the alternative concept of space according to the BSM Supergravitation unified theory,
<http://vixra.org/pdf/1110.0071v1.pdf>
 24. Barry Setterfield
<http://www.journaloftheoretics.com/links/papers/setterfield.pdf>
 25. L. Holmlid, Sub-nanometer distances and cluster shapes in dense hydrogen and in higher levels of hydrogen Rydberg matter by phase-delay spectroscopy, , J. Nanoparticle Research, (2011) 13:5536-5546

26. L. Holmlid, High-energy Coulomb explosions in ultra-dense deuterium: Time-of-flight-mass spectroscopy with variable energy and flight length, International journal of mass spectroscopy 282 (2009) 70-76.
27. F. Olofson, P. U. Andersson and L. Holmlid, Rydberg Matter clusters of alkali metal atoms: the link between meteoritic matter, polar mesosphere summer echoes (PMSE), sporadic sodium layers, polar mesospheric clouds (PMCs, NLCs), and ion chemistry in the mesosphere, (2010) <https://arxiv.org/abs/1002.1570>
28. H. Apsden, IEEE Transactions on Plasma Science, PS-5, 159 (1977).
29. J. D. Sethian, D. A. Hammer and C. B. Wharton, Anomalous Electron-Ion Energy Transfer in a Relativistic-Electron-Beam-Heated Plasma, Physical Review Letters, 40, Number 7, (1978).
30. Yu. Astrov, E. Ammelt, S. Teperick, H. G, Purwins, Hexagonand stripe Turing structures in a gas discharge system, Physics Letters A, , 2011 (1996), 184-190.
31. Yu. Astrov, E. Ammelt, and H. G. Purwins, Experimental Evidence for Zigzag Instability of Solitary Stripes in a Gas Discharge System, Physical Review Letters, 78, 16, (1997), 3129-3132.
32. Stoyan Sarg, Zero Point Energy from the Viewpoint of an Alternative Concept of Space According to the BSM-Supergravitation Unified Theory , <http://vixra.org/pdf/1110.0071v1.pdf>
33. Hick Begich and Jean Manning, *Angels don't play this HAARP*, Earthpulse Press, Alaska, 2007.
34. Morey B. King, *The Energy Machine of T. Henry Moray: Zero-Point Energy and Pulsed Plasma Physics*, \ Paperback – April 10, 2005, amazon.com
35. Joseph Papp noble gas engine,
<http://www.rexresearch.com/papp/1papp.htm>
36. The mystery and legacy of Joseph Papp's noble gas engine, Infinite energy 9 (51), 2003
<https://www.infinite-energy.com/iemagazine/issue51/papp.html>
37. Edwin Grey motor, http://www.free-energy.ws/pdf/ed_gray_bio.pdf
38. Paul Baumann Testatika generator,
<http://www.rexresearch.com/testatik/testart.htm>
39. Testatika video <https://www.youtube.com/watch?v=vOWPJEq42l4>

HIDDEN SPACE ENERGY

40. Testatika pictures <https://rimstar.org/sdenergy/testa/overview.htm>
41. Nag, Amitabh; Rakov, Vladimir A (2012). "Positive lightning: An overview, new observations, and inferences". *JGR: Atmospheres*. **117** (D8): n/a. [Bibcode](#):2012JGRD..117.8109N.
[doi](#):10.1029/2012JD017545.
42. Lightning - slow motion video
<https://www.youtube.com/watch?v=U305Z3IY4pQ>
43. Lightning – slow motion video
<https://www.newsflare.com/video/71456/weather-nature/insane-lightning-strike-in-slow-motion>
44. Lightning – very slow motion video
<https://www.youtube.com/watch?v=dukkO7c2eUE>
45. Lightning – very slow motion video
<https://www.youtube.com/watch?v=W9xzU0xjhE>
46. Parameters of Lightning Strokes: A Review, IEEE Transaction on power delivery, vol. 20, No. 1, January 2005.
47. R. B. Anderson and A. J. Eriksson, Lightning parameters for engineering applications, Electra, no 69, pp 65-102, Mar.1980
48. T. Narita et al., Observation of correct waveshapes of lightning strokes on transmission towers, IEEE Trans. Power delivery, vol. 15, pp429-435, Jan. 2000.
49. *Rocket triggered lightning*
https://www.youtube.com/watch?v=5BJliX9_c_M
50. *Rocket triggered lightning*
<https://www.15min.lt/mokslasit/video/rocket-triggered-lightning-61937>
51. http://www.rakov.ece.ufl.edu/teaching/5490/Properties_II_Section%204b.pdf
52. Biagi, C. J., Jordan, D. M., Uman, M. A., Hill, J. D., Beasley, W. H., and Howard, J. (2009), High-speed video observations of rocket-and-wire initiated lightning, *Geophys. Res. Lett.*, 36, L15801,
53. J. Jerauld et al., A triggered lightning flash containing both negative and positive strokes, GRL, vol 31, L0814, (2004).

54. Editors: C. Guy Suits, Harold E. Way, *The collected work of Irving Langmuir, Vol. 5. Plasma and oscillations*, Pergamon Press, (1961).
55. Yuri P. Raizer, Gas Discharge Physics, (in Russian language, Moscow 1991), Springer-Verlag (English translation, 1991).
56. NASA Scientist Confirms Light Show on Venus
57. Bob Rohner, www.rgenergy.com
<https://www.nasa.gov/vision/universe/solarsystem/venus-20071128.html>
<https://www.space.com/9176-lightning-venus-strikingly-similar-earth.html>
58. Bob Rohner lecture at the ExtraOrdinary Technology Conference (TeslaTech), (2013)
<https://www.youtube.com/watch?v=o-4T8QJ3S0g>
59. Bob Rohner (Roberts-Rohner) video
https://www.youtube.com/watch?v=_zWJNyoFgJM
60. Russ Gries video on Plama pop-p device
<https://www.youtube.com/watch?v=FsvmGcGRf8E>
61. Stoyan Sarg, Atlas of HRM Spectra (Volume 1)
 viXra:1903.0523 *submitted on 2019-03-28*
62. Stoyan Sarg, Heterodyne Resonance Mechanism in a Transient Process in Plasma. Experimental Study and Spectra
<http://viXra:1903.0520> *submitted on 2019-03-28*
63. Stoyan Sarg, Analysis of the HRM Spectra in Plasma Glow Discharge, <http://viXra:1903.0523> *submitted on 2019-03-28*
64. Stoyan Sarg, HRM magnetic features,
<https://www.youtube.com/watch?v=gjQiFzzfZrs>
65. Nag, Amitabh; Rakov, Vladimir A (2012). "Positive lightning: An overview, new observations, and inferences". *JGR: Atmospheres.* **I17** (D8); n/a.
Bibcode:2012JGRD..117.8109N.
doi:10.1029/2012JD017545.
66. M. A. Uman, The lightning discharge. Academic Press, Orlando, FL, 377 pp.

67. J. Jerauld et al., A triggered lightning flash containing both negative and positive strokes, GRL, vol 31, L0814, (2004).
68. Lightning - slow motion video
<https://www.youtube.com/watch?v=U305Z3IY4pQ>
69. Lightning – slow motion video
<https://www.newsflare.com/video/71456/weather-nature/insane-lightning-strike-in-slow-motion>
70. Lightning – very slow motion video
<https://www.youtube.com/watch?v=dukkO7c2eUE>
71. Lightning – very slow motion video
<https://www.youtube.com/watch?v=W9xzU0xjlhE>
72. Parameters of Lightning Strokes: A Review, IEEE Transaction on power delivery, vol. 20, No. 1, January 2005.
73. V. Rakov, CIGRE Technical brochure on lightning parameters for engineering applications,
http://www.rakov.ece.ufl.edu/teaching/5490/Properties_II_Section%204b.pdf
74. R. B. Anderson and A. J. Eriksson, Lightning parameters for engineering applications, Electra, no 69, pp 65-102, Mar.1980
75. T. Narita et al., Observation of correct waveshapes of lightning strokes on transmission towers, IEEE Trans. Power delivery, vol. 15, pp 429-435, Jan. 2000.
76. *Rocket triggered lightning*
https://www.youtube.com/watch?v=5BJliX9_c_M
77. *Rocket triggered lightning*
78. Biagi, C. J., Jordan, D. M., Uman, M. A., Hill, J. D., Beasley, W. H., and Howard, J. (2009), High-speed video observations of rocket-and-wire initiated lightning, *Geophys. Res. Lett.*, 36, L15801.
79. David M. Le Vine, Review of measurements of the RF spectrum of radiation from lightning, NASA Thechnical memorandum 87788 (1986).
80. NASA Scientist Confirms Light Show on Venus
<https://www.nasa.gov/vision/universe/solarsystem/venus-20071128.html>

- <https://www.space.com/9176-lightning-venus-strikingly-similar-earth.html>
81. Stoyan Sarg, (invited keynote speaker). 3rd International Conference on Nano Technology and Materials Science, July 22-24, 2019, Rome, Italy,
<https://www.citationsinternational.com/nanotechnology-conference-2019-rome>
 82. Stoyan Sarg, Study of plasma process in lightning, Rome 2019, Part-1
<https://youtu.be/CrYmtdYmX24>
 83. Stoyan Sarg, Study of lightning ... Rome 2019, Part-2
<https://youtu.be/JSZHY-LZi7A>
 84. Stoyan Sarg, Study of lightning
<https://www.slideshare.net/stoyansarg>
 85. NASA, Exploring the Density of Gas in the Atmosphere,
<https://spacemath.gsfc.nasa.gov/earth/RBSP9.pdf>
 86. J. S. Townsend, The Theory of Ionization of Gases by Collision (Constable, London, 1910). See also J. S. Townsend, Nature 62, 340 (1900); Phil. Mag. 1, 198 (1901).
 87. Henry F. Ivey, Thermionic Electron Emission from Carbon, Physical Review, **76**, 567, (1949).
 88. Energy conversion efficiency
https://en.wikipedia.org/wiki/Energy_conversion_efficiency
 89. Electrification of the clouds
<https://en.wikipedia.org/wiki/Lightning#Electrification>
 90. F. Rinderknecht and Hans-George Herzog, Adaptation and optimization of a linear generator for a hybrid vehicle concept, World electric Vehicle Journal vol. 4 – ISSN 2032-6653, 2010 WEVA
 91. Sandra Eriksson, Uppsala University, Sweden, Design of Permanent-Magnet Linear Generators with Constant-Torque-Angle Control for Wave Power, (2019).
 92. E. R. Williams, Sprites, Eleves,, and Glow Discharge Tubes, Physics Today, November 2001, pp. 41.
 93. S. Badiei and L. Holmlid, Experimental studies of fast fragments of H Rydberg matter, J. Phys. B: At. Mol. Opt. Phys., **39**, (2006) 4191-4212